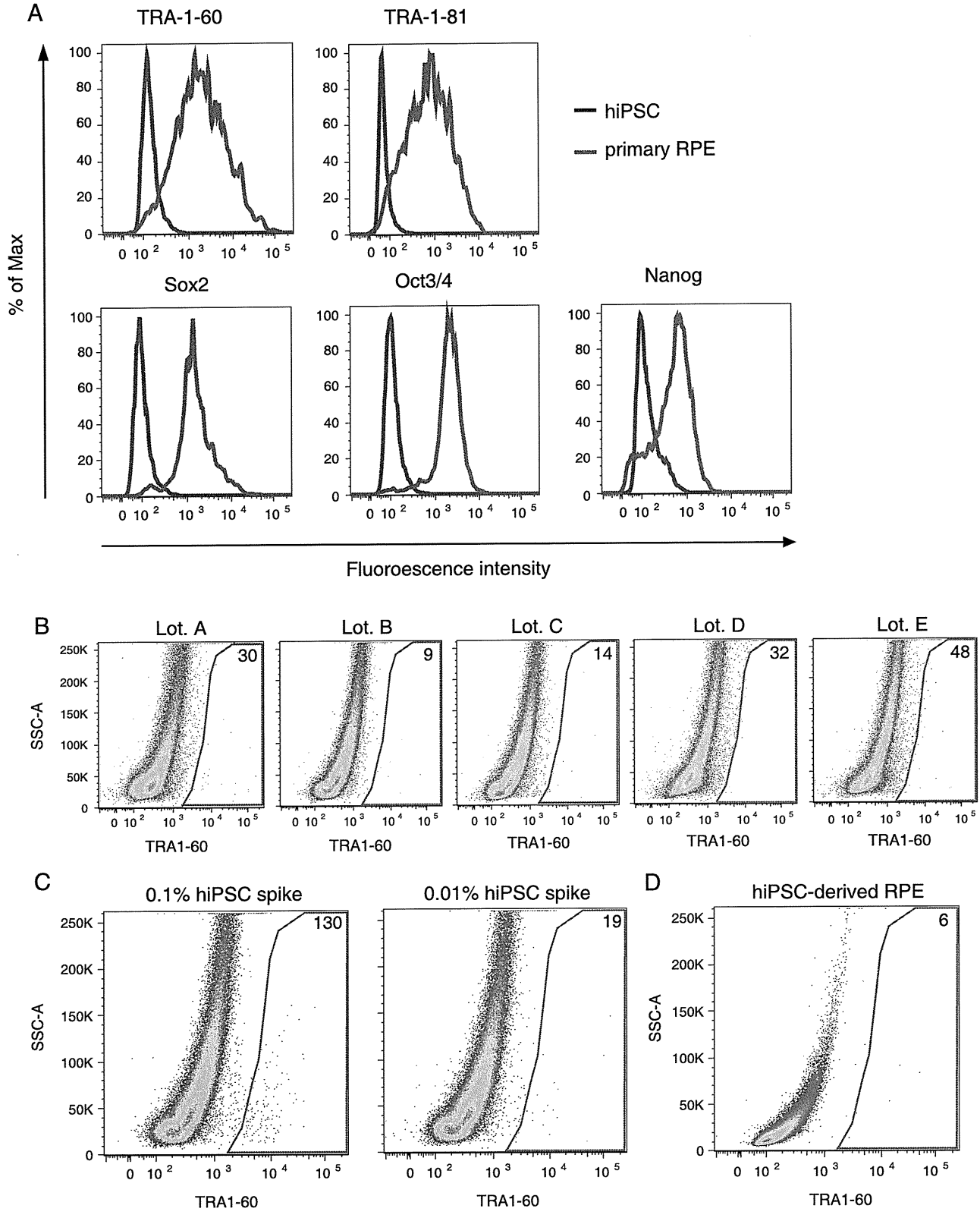

Figure 3. Detection of undifferentiated hiPSCs by flow cytometry assay. (A) Flow cytometry analysis of hiPSCs (blue) and primary RPE cells (red). Cells were fixed, permiabilized and stained with anti-TRA-1-60, anti-TRA-1-81, anti-Sox2, anti-Oct3/4 and anti-Nanog antibodies labeled with fluorophore. (B) Five lots of primary RPE cells were analyzed by flow cytometry with anti-TRA-1-60 antibody. (C) HiPSCs (0.1%, 2.5×10^2 cells; 0.01%, 25 cells) were spiked into primary RPE cells (2.5×10^5 cells) and analyzed by flow cytometry with anti-TRA-1-60 antibody. (D) Flow cytometry analysis of hiPSC-derived RPE cells was performed with anti-TRA-1-60 antibody. Ten thousand cells (A) and 1×10^5 cells (B–D) were used for one assay of flow cytometry analysis. The numbers indicate the quantity of cells contained in the gate.
doi:10.1371/journal.pone.0037342.g003

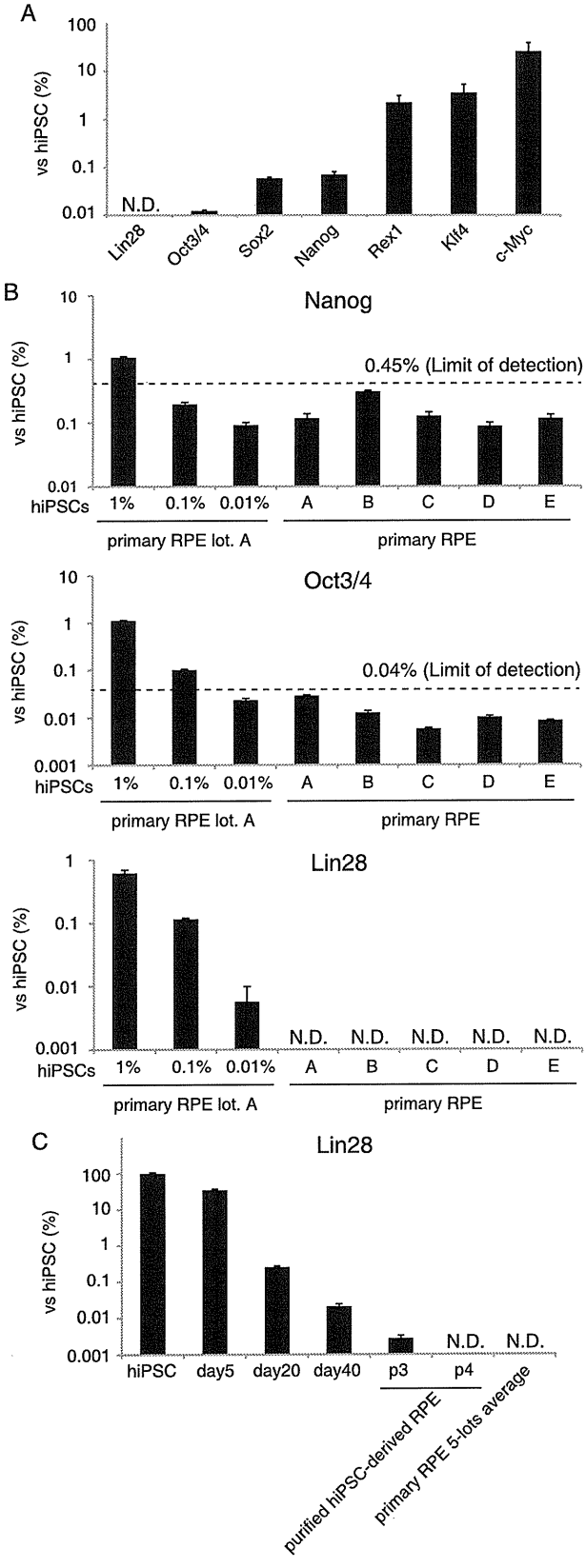

Figure 4. Detection of undifferentiated hiPSCs by qRT-PCR assay. (A) The relative mRNA expressions in primary RPE cells of Lin28, Oct-3/4, Sox2, Nanog, Rex1, Klf4, and c-Myc were determined by qRT-PCR analysis. (B–D) qRT-PCR analysis of hiPSCs spiked into primary RPE cells and five lots of primary RPE cells. Single-cell hiPSCs (1%, 2.5×10^3 cells; 0.1%, 2.5×10^2 cells; 0.01%, 25 cells) were spiked into 2.5×10^5 primary RPE cells, and total RNA was isolated from the mixed cells. The mRNA levels of Nanog (B), Oct3/4 (C) and Lin28 (D) are shown as a relative expression. Limit of detection was calculated as the mean plus 3.3 fold the standard deviation of the measurement of the five lots of primary RPE cells. (E) Lin28 expression of hiPSCs differentiating into RPE and purified hiPSC-derived RPE cells (passage 3 and 4). All values are expressed as mRNA levels relative to those in undifferentiated hiPSCs. Results are means ± standard deviation (n = 3).
doi:10.1371/journal.pone.0037342.g004

poly-D-lysine/gelatin-coated dishes in human ES cell culture medium supplemented with 10 μM Y-27632 (WAKO), 5 μM SB431542 (Sigma–Aldrich) and 3 μM CKI-7 (Sigma–Aldrich) for 1 day. The cells were incubated in a differentiation medium (Glasgow minimum essential medium [GMEM; Invitrogen], 0.1 mM non-essential amino acids, 1 mM sodium pyruvate, and 0.1 mM 2-mercaptoethanol) containing 20% knockout serum replacement (KSR; Invitrogen) for 4 days, then in 15% KSR-containing differentiation medium for 6 days, and finally in 10% KSR-containing differentiation medium for 11–30 days. Y-27632 (10 μM), SB431542 (5 μM) and CKI-7 (3 μM) were added to the differentiation medium for the first 13, 19 and 19 days, respectively. Partially differentiated cells were dissociated with the CTK solution and incubated on non-adhesive dishes (Corning, Corning, NY) in RPE maintenance medium (DMEM:F12 [7:3] supplemented with B-27 supplement [Invitrogen] and 2 mM L-glutamine [Invitrogen]) for 10 days. The resulting RPE cell aggregates were isolated and replated on CELLstart- (Invitrogen) coated dishes in RPE maintenance medium supplemented with 0.5 μM SB431542 and 10 ng/ml bFGF and we defined this stage as passage 1. The medium was changed every 2–3 days.

Soft agar colony formation assay

A soft agar colony formation assay was performed using CytoSelect 96-well Cell Transformation Assay kit (Cell Biolabs, San Diego, CA) according to the manufacturer's instructions with slight modification. Prewarmed 25 μl of 2×DMEM medium containing 20% FBS and 25 μl of 1.2% agar solution were mixed and transferred onto a well of 96-well plates, and then incubated at 4°C for 30 min to allow the bottom agar layer to solidify. Single cell suspensions were prepared as described below: 201B7 cells were dissociated with CTK solution to form cell clumps and incubated on gelatin-coated dishes in the presence of 10 μM Y-27632, a ROCK inhibitor, at 37°C for 1 h to separate with feeder cells. After centrifugation, cell pellets were dissociated into single cells with Accutase (Millipore). Primary RPE cells, hiPSC-derived RPE cells, and PA-1 cells were treated with 0.25% trypsin-EDTA solution (Invitrogen) to dissociate. Cells were passed through 40 μm nylon cell strainers (BD Falcon).

Next, 25 μl of single cell suspensions containing the defined number of cells were mixed with 25 μl of 2×DMEM medium containing 20% FBS and 25 μl of 1.2% agar, and placed on the bottom agar layer. The top agar layers were immediately solidified at 4°C for 10 min to avoid false-positive signals derived from gravity-induced adjacent cells in the agar medium. After the addition of 100 μl of DMEM containing 10% FBS to each well, the plates were incubate for 10, 20 and 30 days at 37°C and 5% CO_2. The medium was changed every 2–3 days. Colonies were lysed and quantified with CyQuant GR dye using a fluorometer equipped with a 485/520 nm filter set (Wallac 1420 ARVOsx mutilabel counter, PerkinElmer, Boston, MA).

Table 1. Comparison of the tumorigenicity-associated assays.

Assay	Soft agar colony formation assay	Flow cytometry	qRT-PCR	*In vivo* tumorigenicity assay using SCID mice (Reference #11)
Measurement standard	Colony formation	Expression of marker protein for pluripotency	Expression of marker gene for pluripotency	Tumor formation
Purpose	Detection of anchorage independent growth	Detection of undifferentiated pluripotent cells	Detection of undifferentiated pluripotent cells	Detection of tumorigenic or undifferentiated pluripotent cells
Time	30 days	1 day	6 hours	12–16 weeks
Advantage	Inexpensive	Rapid	Rapid and simple	Direct
		Analyzing individual cells	Quantitative	Analyzing tumor formation in a specific microenvironment
			High sensitivity	
Disadvantage	Indirect	Indirect	Indirect	Costly
	Not applicable to hiPSCs	Detecting only the cells that express the known maker molecules	Detecting only the cells that express the known marker genes	Time-consuming
		Gating techniques strongly influence the result		
LLOD	1% of PA-1	0.1% of hiPSC (TRA-1-60)	=<0.002% of hiPSC* (Lin28)	245 undifferentiated hESCs with 10^6 feeder fibroblasts (0.025%)

*Not based on the calculation found in Reference #21 because the background signal from the negative controls (primary RPE cells) was not detectable.
doi:10.1371/journal.pone.0037342.t001

qRT-PCR

Total RNA was isolated from cell cultures using an RNeasy Mini Kit (Qiagen, Hilden, Germany) and treated with DNase I according to the manufacturer's instructions. In the spike study, 201B7 cells and RPE cells were mixed at a defined cell number, before total RNA isolation. qRT-PCR was performed with the QuantiTect Probe one-step RT-PCR Kit (Qiagen) on a 7300 Real-Time PCR System (Applied Biosystems, Foster City, CA). The expression levels of target genes were normalized to those of the GAPDH (glyceraldehyde-3-phosphate dehydrogenase) transcript, which were quantified using TaqMan human GAPDH control reagents (Applied Biosystems). Probes and primers were obtained from Sigma–Aldrich. The sequences of primers and probes used in the present study are listed in Table S1. All qRT-PCR reactions were run at 45 cycles.

Flow Cytometry

201B7 cells and RPE cells were dissociated into single cells as described above. Cells were fixed with the BD Cytofix fixation buffer (BD Biosciences, Bedford, MA) for 20 min and permeabilized with BD Perm/Wash buffer (BD Biosciences) for 10 min at room temperature. Cells were incubated for 1 h at room temperature with the following primary antibodies and fluorochrome-conjugated antibodies: mouse anti-CRALBP monoclonal 1:1000 (B2, Thermo Scientific, Roskilde, Denmark); rabbit anti-GP-100 monoclonal 1:1000 (P14-V, Enzo Life Sciences, Lausen, Switzerland); FITC mouse anti-TRA-1-60 monoclonal 1:5 (TRA-1-60, BD Pharmingen); PE mouse anti-TRA-1-81 monoclonal 1:5 (TRA-1-81, BD Pharmingen); PerCP-Cy5.5 mouse anti-Oct3/4 monoclonal 1:5 (40/Oct-3, BD Pharmingen); Alexa Fluor 647 mouse anti-Sox2 monoclonal 1:5 (245610, BD Pharmingen); PE mouse anti-Nanog monoclonal 1:5 (N31–355, BD Pharmingen). Indirect immunostaining was then completed with either donkey-anti-mouse or donkey-anti-rabbit Alexa Fluor 647-conjugated secondary antibodies 1:1000 (Molecular Probes) for 1 h. Appropriate antibodies were used as a negative control. To obtain fluorescein-labeled hiPSCs, 201B7 cells were incubated with 10 μM carboxyfluorescein diacetate succinimidyl ester (CFDA; Invitrogen) in phosphate buffered saline (PBS) for 8 min, dissociated into a single cell suspension, and then fixed as described above. Stained cells were analyzed with a BD FACSAria II (BD Biosciences). Data retrieved from the sorting was analyzed with Flowjo software 9.3.3 (Tree Star, Ashland, OR).

Immunocytochemistry

All manipulations were performed at room temperature. Cultured primary and hiPSC-derived RPE cells were fixed with 4% paraformaldehyde in PBS for 20 min at room temperature. After washing with PBS, the cells were permeabilized with 0.2% Triton-X100 in PBS for 15 min and blocked with 2% bovine serum albumin in PBS for 30 min. Samples were incubated for 1 h with mouse anti-N-cadherin monoclonal antibody 1:1000 (GC-4, Sigma–Aldrich). The cells were washed with PBS and incubated with 1:1000 Alexa Fluor 488 F(ab')2 fragment of goat anti-mouse IgG 1:1000 (Molecular Probes) for 1 h. The samples were mounted with a Vectashield mounting medium containing DAPI (Vector Laboratories, Burlingame, CA) and examined with a Biozero-8000 fluorescence microscope (Keyence, Japan).

Supporting Information

Figure S1 Soft agar colony formation assay of hiPSCs, teratocarcinoma PA-1 cells and primary RPE cells. (A) hiPSCs (10000 cells, 6000cells and 3000 cells/well) were grown in soft agar for 10, 20 and 30 days with 10 μM Y-27632. (B) PA-1 cells (1000, 500, 300, 200, 100, 50, 30 cells/well) were grown in soft agar for 20 days. (C) Primary RPE cells (lot. A, 100,000, 60,000, 30,000 and 10,000 cells/well) were grown in soft agar for 30 days. (A–C) Cell growth was quantified using a CytoSelect kit and the results expressed as a relative fold change of the value of a blank well. Error bars represent the standard deviation of the measurements (n = 3).
(EPS)

Figure S2 Flow cytometry analysis of spiked hiPSCs cells in primary RPE. CFDA-stained hiPSCs (1%, 2,500 cells; 0.1%, 250 cells; 0.01%, 25 cells) were spiked into primary RPE (2.5×10^5 cells) and 1×10^5 cells were analyzed by flow cytometry. The numbers indicate the quantity of cells contained in the gate. (EPS)

Table S1 Probes and primers for qRT-PCR. (DOCX)

Acknowledgments

We would like to thank Masahiro Go, Hoshimi Kanemura and Akifumi Matsuyama for their valuable discussion on this paper. We also thank Satoshi Okamoto and Noriko Sakai for technical advice of RPE cell differentiation.

Author Contributions

Conceived and designed the experiments: TK SY YS. Performed the experiments: TK SY NH. Analyzed the data: TK SY S. Kusakawa NH YK KS MT SN S. Kawamata YS. Contributed reagents/materials/analysis tools: YK MT S. Kawamata. Wrote the paper: TK SY YS. Acquired the funding: SN S. Kawamata KS YS.

References

1. Thomson JA, Itskovitz-Eldor J, Shapiro SS, Waknitz MA, Swiergiel JJ, et al. (1998) Embryonic stem cell lines derived from human blastocysts. Science 282: 1145–1147.
2. Takahashi K, Tanabe K, Ohnuki M, Narita M, Ichisaka T, et al. (2007) Induction of pluripotent stem cells from adult human fibroblasts by defined factors. Cell 131: 861–872.
3. Kehat I, Kenyagin-Karsenti D, Snir M, Segev H, Amit M, et al. (2001) Human embryonic stem cells can differentiate into myocytes with structural and functional properties of cardiomyocytes. J Clin Invest 108: 407–414.
4. Zhang SC, Wernig M, Duncan ID, Brustle O, Thomson JA (2001) *In vitro* differentiation of transplantable neural precursors from human embryonic stem cells. Nat Biotechnol 19: 1129–1133.
5. Cai J, Zhao Y, Liu Y, Ye F, Song Z, et al. (2007) Directed differentiation of human embryonic stem cells into functional hepatic cells. Hepatology 45: 1229–1239.
6. Song Z, Cai J, Liu Y, Zhao D, Yong J, et al. (2009) Efficient generation of hepatocyte-like cells from human induced pluripotent stem cells. Cell Res 19: 1233–1242.
7. Osakada F, Jin ZB, Hirami Y, Ikeda H, Danjyo T, et al. (2009) *In vitro* differentiation of retinal cells from human pluripotent stem cells by small-molecule induction. J Cell Sci 122: 3169–3179.
8. Carr AJ, Vugler AA, Hikita ST, Lawrence JM, Gias C, et al. (2009) Protective effects of human iPS-derived retinal pigment epithelium cell transplantation in the retinal dystrophic rat. PLoS One 4: e8152.
9. Ben-David U, Benvenisty N (2011) The tumorigenicity of human embryonic and induced pluripotent stem cells. Nat Rev Cancer 11: 268–277.
10. Knoepfler PS (2009) Deconstructing stem cell tumorigenicity: a roadmap to safe regenerative medicine. Stem Cells 27: 1050–1056.
11. Hentze H, Soong PL, Wang ST, Phillips BW, Putti TC, et al. (2009) Teratoma formation by human embryonic stem cells: evaluation of essential parameters for future safety studies. Stem Cell Res 2: 198–210.
12. Lee AS, Tang C, Cao F, Xie X, van der Bogt K, et al. (2009) Effects of cell number on teratoma formation by human embryonic stem cells. Cell Cycle 8: 2608–2612.
13. Noaksson K, Zoric N, Zeng X, Rao MS, Hyllner J, et al. (2005) Monitoring differentiation of human embryonic stem cells using real-time PCR. Stem Cells 23: 1460–1467.
14. Pera MF, Reubinoff B, Trounson A (2000) Human embryonic stem cells. J Cell Sci 113(Pt 1): 5–10.
15. Draper JS, Pigott C, Thomson JA, Andrews PW (2002) Surface antigens of human embryonic stem cells: changes upon differentiation in culture. J Anat 200: 249–258.
16. Van Aken EH, De Wever O, Van Hoorde L, Bruyneel E, De Laey JJ, et al. (2003) Invasion of retinal pigment epithelial cells: N-cadherin, hepatocyte growth factor, and focal adhesion kinase. Invest Ophthalmol Vis Sci 44: 463–472.
17. Hamburger AW, Salmon SE (1977) Primary bioassay of human tumor stem cells. Science 197: 461–463.
18. Watanabe K, Ueno M, Kamiya D, Nishiyama A, Matsumura M, et al. (2007) A ROCK inhibitor permits survival of dissociated human embryonic stem cells. Nat Biotechnol 25: 681–686.
19. Ohgushi M, Matsumura M, Eiraku M, Murakami K, Aramaki T, et al. (2010) Molecular pathway and cell state responsible for dissociation-induced apoptosis in human pluripotent stem cells. Cell Stem Cell 7: 225–239.
20. Albini A, Iwamoto Y, Kleinman HK, Martin GR, Aaronson SA, et al. (1987) A rapid *in vitro* assay for quantitating the invasive potential of tumor cells. Cancer Res 47: 3239–3245.
21. Miller JNMJC (2005) Statistics and Chemometrics for Analytical Chemistry Fifth edition. Harlow: Person Education Limited.
22. Andrews PW, Banting G, Damjanov I, Arnaud D, Avner P (1984) Three monoclonal antibodies defining distinct differentiation antigens associated with different high molecular weight polypeptides on the surface of human embryonal carcinoma cells. Hybridoma 3: 347–361.
23. Nakagawa M, Koyanagi M, Tanabe K, Takahashi K, Ichisaka T, et al. (2008) Generation of induced pluripotent stem cells without Myc from mouse and human fibroblasts. Nat Biotechnol 26: 101–106.
24. Okita K, Hong H, Takahashi K, Yamanaka S (2010) Generation of mouse-induced pluripotent stem cells with plasmid vectors. Nat Protoc 5: 418–428.
25. Maekawa M, Yamaguchi K, Nakamura T, Shibukawa R, Kodanaka I, et al. (2011) Direct reprogramming of somatic cells is promoted by maternal transcription factor Glis1. Nature 474: 225–229.
26. Tang C, Lee AS, Volkmer JP, Sahoo D, Nag D, et al. (2011) An antibody against SSEA-5 glycan on human pluripotent stem cells enables removal of teratoma-forming cells. Nat Biotechnol 29: 829–834.
27. Levenbook IS, Petricciani JC, Qi Y, Elisberg BL, Rogers JL, et al. (1985) Tumorigenicity testing of primate cell lines in nude mice, muscle organ culture and for colony formation in soft agarose. J Biol Stand 13: 135–141.
28. Nam Y, Chen C, Gregory RI, Chou JJ, Sliz P (2011) Molecular Basis for Interaction of let-7 MicroRNAs with Lin28. Cell 147: 1080–1091.
29. West JA, Viswanathan SR, Yabuuchi A, Cunniff K, Takeuchi A, et al. (2009) A role for Lin28 in primordial germ-cell development and germ-cell malignancy. Nature 460: 909–913.

nature COMMUNICATIONS

ARTICLE

Received 30 Jul 2012 | Accepted 29 Oct 2012 | Published 4 Dec 2012

DOI: 10.1038/ncomms2231

OPEN

Laminin E8 fragments support efficient adhesion and expansion of dissociated human pluripotent stem cells

Takamichi Miyazaki[1], Sugiko Futaki[2], Hirofumi Suemori[1], Yukimasa Taniguchi[2], Masashi Yamada[2], Miwa Kawasaki[2], Maria Hayashi[2], Hideaki Kumagai[1], Norio Nakatsuji[3,4], Kiyotoshi Sekiguchi[2] & Eihachiro Kawase[1]

Human embryonic stem cells (hESCs) and induced pluripotent stem cells (hiPSCs) have the potential to provide an infinite source of tissues for regenerative medicine. Although defined xeno-free media have been developed, culture conditions for reliable propagation of hESCs still require considerable improvement. Here we show that recombinant E8 fragments of laminin isoforms (LM-E8s), which are the minimum fragments conferring integrin-binding activity, promote greater adhesion of hESCs and hiPSCs than do Matrigel and intact laminin isoforms. Furthermore, LM-E8s sustain long-term self-renewal of hESCs and hiPSCs in defined xeno-free media with dissociated cell passaging. We successfully maintained three hESC and two hiPSC lines on LM-E8s in three defined media for 10 passages. hESCs maintained high level expression of pluripotency markers, had a normal karyotype after 30 passages and could differentiate into all three germ layers. This culture system allows robust proliferation of hESCs and hiPSCs for therapeutic applications.

[1] Department of Embryonic Stem Cell Research, Institute for Frontier Medical Sciences, Kyoto University, 53 Kawahara-cho, Shogoin, Sakyo-ku, Kyoto 606-8507, Japan. [2] Laboratory of Extracellular Matrix Biochemistry, Institute for Protein Research, Osaka University, 3-2 Yamadaoka, Suita, Osaka 565-0871, Japan. [3] Department of Development and Differentiation, Institute for Frontier Medical Sciences, Kyoto University, 53 Kawahara-cho, Shogoin, Sakyo-ku, Kyoto 606-8507, Japan. [4] Institute for Integrated Cell-Material Sciences (WPI-iCeMS), Kyoto University, Ushinomiya-cho, Yoshida, Sakyo-ku, Kyoto 606-8501, Japan. Correspondence should be addressed to E.K. (email: kawase8@frontier.kyoto-u.ac.jp) for general correspondence or K.S. (email: sekiguch@protein.osaka-u.ac.jp) for recombinant laminin products.

Human embryonic stem cells (hESCs) and induced pluripotent stem cells (hiPSCs) have great potential for a wide range of applications in regenerative medicine, and as tools for human disease modelling and drug discovery. However, defined xeno-free and feeder-free systems have not been fully established for the realization of these applications. Several types of defined medium have been developed, which consist of known components and avoid the use of animal products[1–5]. However, the widespread use of Matrigel as a culture substrate is potentially problematic[6]. Matrigel is not an optimal substrate because it is derived from mouse Engelbreth–Holm–Swarm tumours and contains many unknown components. Additionally, hESCs usually propagate as colonies in culture, and their passaging involves either enzymatic dissociation by gently pipetting or manual microdissection of the cells[7]. hESC colonies grow as a monolayer and sustain an undifferentiated state, whereas the formation of large aggregates during passaging accelerates their spontaneous differentiation. Thus, it is somewhat difficult to precisely control appropriate dissociation of hESCs while passaging. As a result, conventional colony-based protocols often have considerable variations in culture outcomes. One method to overcome such difficulties might be complete dissociation of hESCs by an optimized and standardized protocol. However, complete dissociation of hESC clumps into single cells causes extensive cell death, and the survival is generally $<1\%$ (refs 8,9). Furthermore, complete cell dissociation is thought to be associated with an increased risk of karyotypic abnormalities[10,11]. In this study, we aimed to identify an optimal substrate with the greatest adhesive property for the culture of completely dissociated hESCs and hiPSCs, and we further examined whether it could promote robust propagation of these cells while retaining a normal karyotype.

Although there are reports of the replacement of Matrigel with defined substrates, such as small peptides, to allow sustained hESC self-renewal in defined or xeno-free media[3–5,12–18], considerable improvements and refinements of these substrates are still needed. Laminin, the main component of Matrigel, is a heterotrimeric glycoprotein composed of three covalently linked chains that are termed α, β and γ[19].Thus far, 15 laminin isoforms formed by various combinations of each chain (α1–α5, β1–β3 and γ1–γ3) have been identified. We have previously shown that human recombinant laminin isoforms (laminin-511, -332 and -111) support hESC proliferation in an undifferentiated state, although laminin-111 shows weak cell adhesive properties[20]. Laminin-511, the first and only alternative substrate with a greater adhesive property for hESCs than that provided by Matrigel, also permits sustained self-renewal of hESCs in xeno-free culture conditions[12]. Typically, procedures for the isolation of native pure laminins from tissues are arduous or highly impractical. Recently, some recombinant laminins have been produced using mammalian expression systems[21–25]. However, full-length laminins are large heterotrimeric proteins (Fig. 1a), and mass production of these recombinant proteins is still very difficult. Therefore, we examined whether recombinant laminin fragments could support adhesion and undifferentiated proliferation of hESCs and hiPSCs. These fragments are obviously smaller molecules and have a much higher yield compared with that of the full-length protein.

Laminin isoforms bind to multiple receptors on the cell surface, including integrins, syndecans and dystroglycans, of which integrins serve as the major adhesion receptors of hESCs[26]. Laminin-511, -332 and -111 share the characteristic of specific high affinity for α6β1 integrin[27]. Using function-blocking antibodies, α6β1 integrin has been identified as the major cell adhesion receptor for both Matrigel and laminin-511 (refs 12,28). Furthermore, α6β1 integrin is abundantly expressed by both hESCs[20] and hiPSCs (Supplementary Fig. S1). Thus, we examined whether the integrin-binding site in laminin is solely necessary for the maintenance of hESCs and hiPSCs.

Laminin E8 fragments (LM-E8s) are truncated proteins composed of the C-terminal regions of the α, β and γ chains. These truncated proteins contain the active integrin-binding site comprising the laminin globular 1-3 domains of the α chain[21] and the glutamate residue in the C-terminal tail of the γ chain[29], but lack other activities such as the heparin/heparan sulphate-binding activity, which are associated with intact laminins[21]. Therefore, LM-E8s serve as a functionally minimal form that retains the full capability for binding to α6β1 integrin[30]. When LM-E8s are separated into an α chain and a disulphide-bonded dimer of β and γ chains, they lose their cell adhesive activity[31], underscoring the requirement for all three chains for their integrin-binding activity. Thus, the integrin-binding site of laminin appears to be a composite epitope composed of multiple polypeptides[32], thereby making it difficult to recapitulate the integrin-binding site with synthetic peptides modelled on individual laminin subunits.

In this study, we produced two recombinant LM-E8s, LM511-E8 from laminin-511 and LM332-E8 from laminin-332, both of which have high cell adhesive properties (Fig. 1a), and examined their capabilities as adhesion substrates for hESCs and hiPSCs. Both fragments display stronger adhesion affinities for hESCs and hiPSCs than those of other substrates. Furthermore, LM-E8s enable robust propagation of hESCs and hiPSCs in an undifferentiated state in cultures with defined and xeno-free media using dissociated cell passaging.

Results

LM-E8s maximize hESC and hiPSC adhesion. Extracellular matrix (ECM) proteins vary considerably in their affinities for receptors, and in protein size and charge. Consequently, different proteins vary in their optimal use as a cell culture support matrix. To determine whether LM511-E8 and LM332-E8 were suitable for hESC and hiPSC adhesion, we first compared the adhesive properties of completely dissociated H9 hESCs and iPS(IMR90)-1 cells in mTeSR1 medium on matrices containing LM511-E8 or LM332-E8 with those on other matrices. Cell adhesion on all matrices showed dose-dependent increases, but with different maxima: 15 $\mu g\,cm^{-2}$ for Matrigel; 3–6 $\mu g\,cm^{-2}$ for intact laminin-511 and -332; and 1.5 $\mu g\,cm^{-2}$ for LM511-E8 and LM332-E8 (Fig. 1b and Supplementary Figs S2a and S3a). In agreement with a previous report[12], adhesion to intact laminin-511 or -332 was higher than that to Matrigel. However, we found that LM511-E8 and LM332-E8 had significantly higher adhesive properties than those of intact laminin-511 and -332. We therefore used LM511-E8 and LM332-E8 at a coating concentration of 1.5 $\mu g\,cm^{-2}$ in subsequent experiments.

To confirm that LM511-E8 and LM332-E8 were recognized by α6β1 integrin on the cell surface, we used integrin function-blocking antibodies to investigate whether α6 and/or β1 integrins were required for the adhesion of H9 hESCs to LM-E8-coated substrata in mTeSR1 medium (Fig. 1c; Statistical results of multiple comparisons are shown in Supplementary Tables S1a and S1b). Cell attachment to both LM-E8s was significantly reduced by the addition of antibodies against α6 and/or β1 integrins. We further confirmed that an inactive form of LM511-E8 (LM511(EQ)), in which the glutamic acid residue (E) at the third position from the C-terminus in the γ chain was replaced by a glutamine residue (Q)[29], showed dramatic abrogation of cell adhesion (Fig. 1c). Taken together, these data showed that α6β1 integrin mediated the adhesion of completely dissociated hESCs to LM511-E8 and LM332-E8.

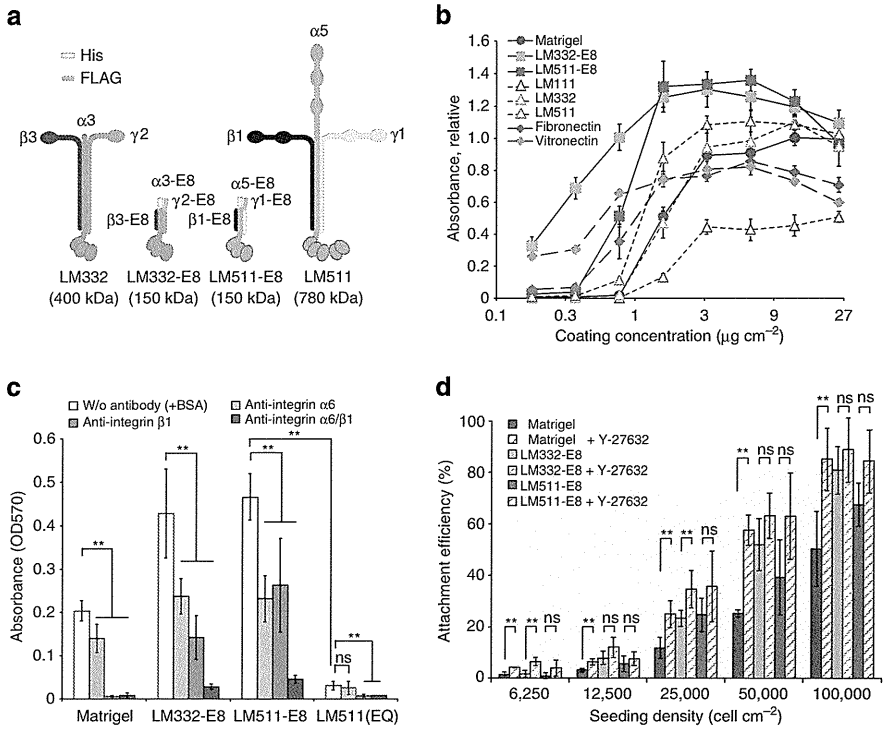

Figure 1 | Validation of LM-E8s for H9 hESC attachment. (**a**) Schematic representations of the two LM-E8s and the original intact laminin isoforms. A 6xHis-tag and FLAG-tag were attached to the N-termini of the α and γ chains, respectively, of LM-E8s to facilitate the purification of recombinant LM-E8s. The molecular weights of individual proteins are shown in parentheses. (**b**) Dose-response adhesion curves of H9 hESCs on various ECMs. LM-E8s at 1.5 μg cm^{-2} showed higher efficiency for supporting the adhesion of dissociated cells than did other matrices. The means of absorbance (OD570) represent the relative number of adherent cells normalized against the values at the maximum effect on Matrigel, which was arbitrarily set as 1. Error bars show the s.e.m. of five independent assays, except for vitronectin, which shows the average of duplicate assays. (**c**) Inhibition of integrins on LM-E8s. Completely dissociated H9 hESCs were incubated with an integrin-specific blocking antibody for 30 min in mTeSR1 medium. LM511(EQ): an inactive form of LM511-E8. Error bars indicate the s.d. of five individual assays. $^{**}P<0.05$; ns, non-significant; two-way ANOVA or Tukey's test. (**d**) Seeding density-dependent adhesion of H9 hESCs on LM-E8s. LM-E8s showed a higher cell adhesive activity for completely dissociated H9 hESCs than did Matrigel. Completely dissociated cells were incubated on LM-E8s in mTeSR1 medium for 6 h with or without Y-27632. Data represent the means ± s.d. of three experiments. $^{**}P<0.05$; ns, non-significant, two-tailed Student's *t*-test.

Both LM332-E8 and LM511-E8 showed higher adhesion for completely dissociated hESCs or hiPSCs than did Matrigel at various cell densities (Fig. 1d and Supplementary Fig. S3b). Furthermore, using the optimal cell density (more than 50,000 cells per cm^2), we observed attachment of 40–70% of cells to LM-E8s, which raised the possibility of passaging cultures by completely dissociating hESCs and hiPSCs.

It has been previously shown that the Rho-associated protein kinase (ROCK) inhibitor Y-27632 increases the adhesion of dissociated hESCs[33]. However, the effect of Y-27632 on hESC and hiPSC cultures in LM-E8-coated plates was unclear (Fig. 1d and Supplementary Fig. S3b). Y-27632 pretreatment before complete dissociation did not significantly improve the attachment of dissociated H9 hESCs on LM-E8s (Supplementary Fig. S2b). We therefore concluded that the addition of Y-27632 to the medium was unnecessary for cultures using LM-E8s, unlike attachment onto Matrigel, fibronectin, vitronectin and Synthemax that has a synthetic culture surface consisting of short peptides derived from vitronectin (Supplementary Fig. S2c). To focus on the effectiveness of LM-E8s, we did not use Y-27632 in subsequent experiments. In addition, we selected 50,000 cells per cm^2 as the seeding density for passaging hESCs and hiPSCs.

LM-E8s support vigorous proliferation in defined media. We next examined whether LM-E8s supported undifferentiated growth of completely dissociated hESCs and hiPSCs in mTeSR1 medium. H9 hESC colonies dissociated by a conventional method showed superior attachment to LM-E8s (Fig. 2a). Likewise, completely dissociated H9 hESCs showed strong adherence on LM-E8s. Cells quickly adhered and spread on LM-E8-coated substrates, with extending lamellipodium-like protrusions (Fig. 2b and Supplementary Movies 1 and 2). H9 hESCs adhered to LM-E8s promptly recovered cell–cell contacts, formed highly dense colonies (Fig. 2c), and showed steady proliferation similar to that of conventional colony cultures (Fig. 2d). Similarly, completely dissociated iPS(IMR90)-1 cells also exhibited steady proliferation on LM-E8 fragments (Supplementary Fig. S3c). In contrast, completely dissociated H9 hESCs displayed weak adhesion on Matrigel or considerably poor adhesion on fibronectin and vitronectin, although H9 hESC colonies normally adhere to these substrates (Fig. 2a). Most dissociated cells on Matrigel, fibronectin and vitronectin remained as single cells and rapidly underwent cell death (Fig. 2b and Supplementary Movies 3–5). In agreement with the cell adhesion and survivability on LM-E8s, molecular analysis revealed that LM-E8s stimulated the signalling pathways downstream of integrins in hESCs and iPSCs. AKT, FAK and ERK1/2, signalling molecules closely associated with cell survival and migration[34], were activated to a greater extent in cells cultured on LM-E8s than in cells cultured on fibronectin or vitronectin (Fig. 2e). Y-27632 treatment abrogated MLC2 phosphorylation regardless of culture substrates, indicating that

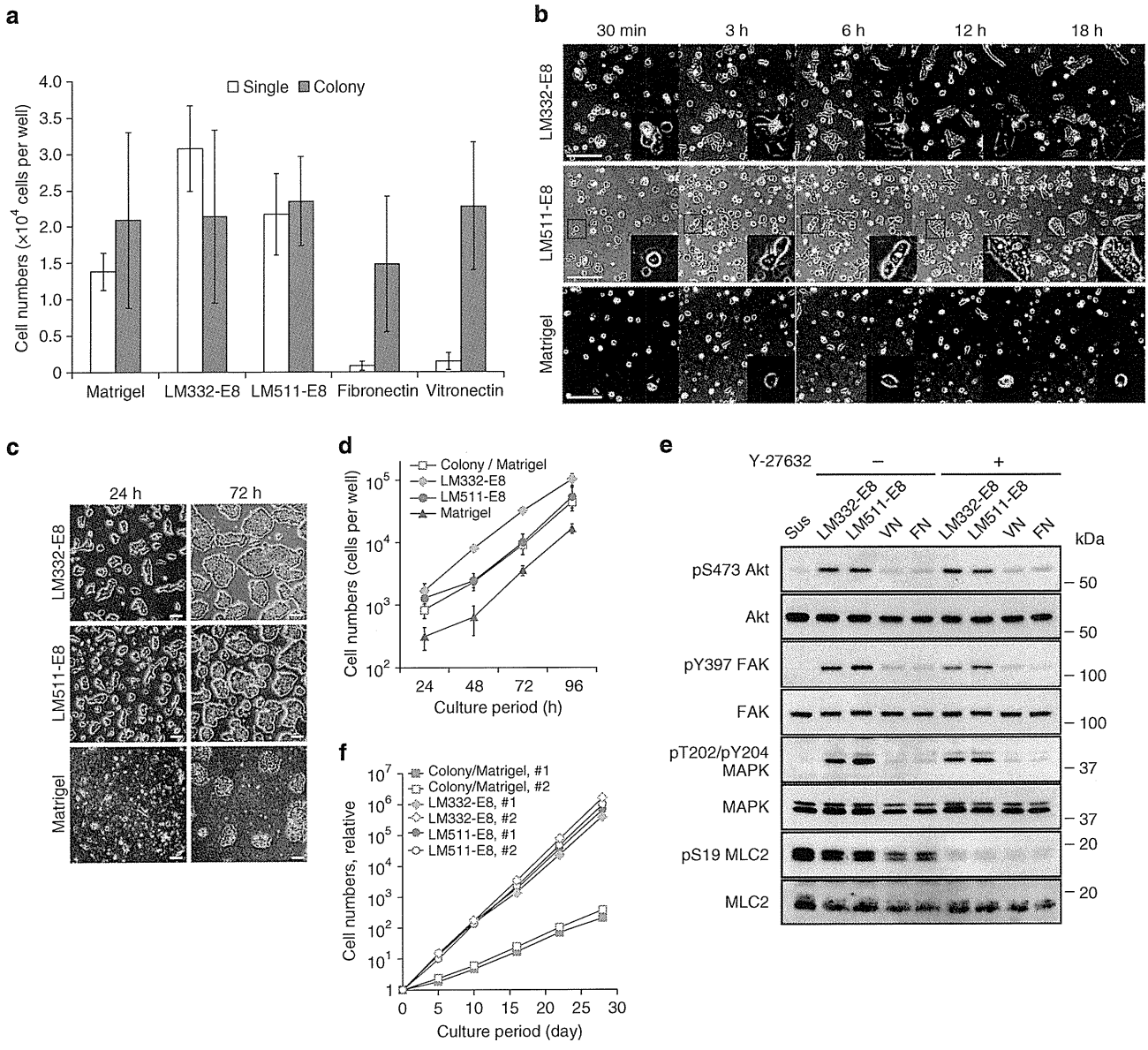

Figure 2 | LM-E8s support undifferentiated proliferation in defined medium. (**a**) Distinct cell survival of H9 hESCs depending on ECMs. Data represent the numbers of live cells at 24 h after seeding 3.75×10^4 cells as single cells (single) or colonies (colony). (**b**) Serial phase-contrast images of H9 hESCs on LM-E8s or Matrigel in mTeSR1 medium at initial attachment. Images at the bottom right show an enlarged view of enclosed boxes. Note that dissociated H9 hESCs promptly extended and reached neighbouring cells on LM-E8s, but failed cellular extension on Matrigel. See also Supplementary Movies 1-5. (**c**) Phase-contrast images of H9 hESCs in mTeSR1 medium on LM-E8s or Matrigel during the growth phase. (**d**) Short-term growth curves of H9 hESCs on LM-E8s in mTeSR1 medium. Dissociated H9 hESCs on LM-E8s proliferated and had a similar growth rate as that in conventional colony culture during logarithmic growth. Data represent the means ± s.d. of three individual experiments. (**e**) Detection of phosphorylated proteins associated with cell adhesion by western blot analysis. Cell lysates were prepared from H9 hESCs incubated for 1 h on each substrate with or without Y-27632. Sus, dissociated H9 hESCs incubated for 1 h in suspension; FN, fibronectin; VN, vitronectin. (**f**) Long-term growth curves of H9 hESCs on LM-E8s in mTeSR1 medium. The numbers of seeded cells at the initial passage were converted to 1, and the counted cell numbers at each passage are shown as cumulative cell numbers. Note that dissociation culture on LM-E8s resulted in a more than 200-fold increase in cell numbers relative to conventional colony culture over 1 month. Scale bars, 200 μm.

the signalling pathways promoting cell survival on LM-E8s were not the same as those targeted by Y-27632. Once H9 hESCs adhered on each culture substrate, the cells similarly proliferated at an invariable rate that was regardless of the culture substrate, cluster size and Y-27632 treatment (Fig. 2d and Supplementary Fig. S2d). Therefore, the expansion efficiency was simply dependent on the initial adhesion efficiency and passaging ratio. LM-E8s allowed a higher passaging ratio during subculture, which was approximately 1:10 compared with 1:4 for conventional colony culture. Indeed, LM-E8s yielded more than 200-fold of the number of cells compared with that obtained by conventional culture over a 1-month period (Fig. 2f). Thus, LM-E8s enabled rapid expansion of completely dissociated hESCs and hiPSCs by supporting robust adhesion and rapid cell expansion.

Using our culture protocol with LM-E8s and two chemically defined media (mTeSR1 and StemPro), three hESC lines (H9, HES3 and KhES-1) and two hiPSC lines (iPS(IMR90)-1 and 253G1) showed robust proliferation for at least 10 serial passages. Flow cytometric analysis further indicated that the majority of dissociated hESCs and hiPSCs cultured on LM-E8s

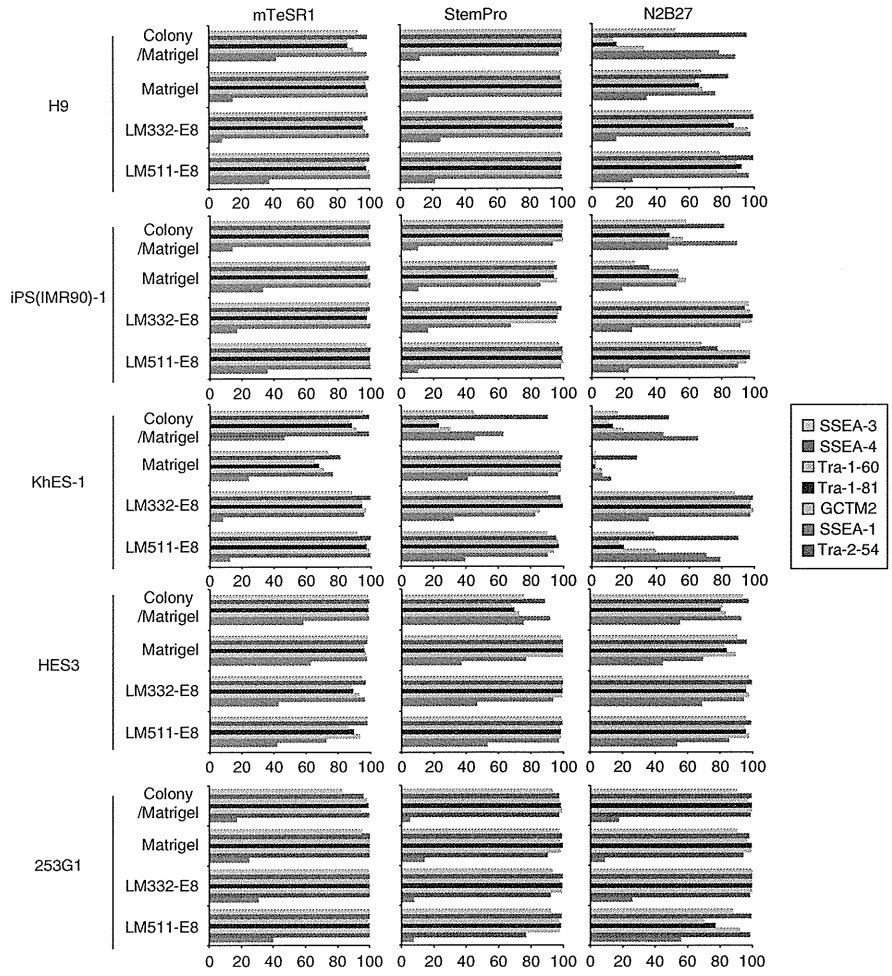

Figure 3 | Flow cytometric analysis of hESC or hiPSC lines. Three hESC lines (H9, HES3 and KhES-1) and two hiPSC line (iPS(IMR90)-1 and 253G1) were cultured on LM-E8s after complete dissociation. These cells maintained higher expression levels of the undifferentiated markers, compared with that on Matrigel with either colony or complete dissociation culture. Undifferentiated markers: SSEA-3, SSEA-4, Tra-1-60, Tra-1-81, GCTM2 and Tra-2-54. Differentiation marker: SSEA-1. Data were collected from cells cultured for 10 passages. The percentages of positive cells are indicated on the graph.

expressed pluripotency markers SSEA-3, SSEA-4, Tra-1-60, Tra-1-81, GCTM2 and Tra-2-54, with only low level of expression of the differentiation marker SSEA-1 (Fig. 3). It has been reported that N2B27 medium is less robust for hESC maintenance, compared with two other media[2], but almost all hESCs and hiPSCs, except for KhES-1, cultured on LM-E8s showed undifferentiated growth in N2B27 medium. We karyotyped 50 randomly selected cells after G-banding of each cell line for all experiments at passage 10. Cells propagated on LM-E8s after complete dissociation had normal karyotypes (Table 1 and Supplementary Fig. S4a, b). Using multiplex fluorescence *in situ* hybridization (M-FISH) analysis, we showed that completely dissociated H9 hESCs and iPS(IMR90)-1 cells had a normal karyotype after 30 and 20 passages on LM-E8s, respectively (Supplementary Fig. S4c–f).

To assess the pluripotency of hESCs that had been cultured on LM-E8s in mTeSR1 medium for 10 passages, the cells were treated with the growth factors described in the Methods. We found that hESCs could differentiate into ectoderm (βIII tubulin), mesoderm (α-smooth muscle actin) or endoderm (α-fetoprotein), as determined by immunohistochemical analyses (Fig. 4a). Furthermore, reverse transcriptase PCR (RT–PCR) analysis showed that, when hESCs were placed in suspension culture, they formed embryoid bodies with increased expression of gene markers for all three germ layer lineages after 10 days of incubation (Fig. 4b). Similar results were obtained for iPS (IMR90)-1 cells cultured on LM-E8s (Supplementary Fig. S5). We further confirmed that hESCs cultured on LM-E8s in mTeSR1 medium for 25 passages formed teratomas consisting of all three germ layers, including neuroepithelium (ectoderm), intestinal epithelium (endoderm) and cartilage (mesoderm) (Fig. 4c).

Thus, our new culture method using completely dissociated cells on LM-E8s supported long-term maintenance and efficient cell expansion of hESCs and hiPSCs in an undifferentiated state.

LM-E8s support vigorous proliferation in xeno-free medium. The final goal of this study was to characterize LM-E8s as substrates that support hESCs in a sustainable undifferentiated state under a xeno-free culture condition. We cultured completely dissociated H9 hESCs and 253G1 iPSCs on LM511-E8 or LM332-E8 in TeSR2 medium that is chemically defined and animal protein free. Dissociated H9 hESCs tightly adhered on LM-E8s in TeSR2 medium (Fig. 5a). Similarly to the results described for defined media, we found that H9 hESCs and 253G1 iPSCs proliferated robustly for more than 30 and 10 passages, respectively. Flow cytometric analysis also confirmed that the cells retained their undifferentiated state (Fig. 5b and Supplementary Fig. S6a). RT–PCR analysis of H9 hESCs and 253G1 iPSCs

Table 1 | Summary of karyotypic analysis.

Cell line	Medium	Colony culture	Matrigel	LM332-E8	LM511-E8
H9	mTeSR1	Normal*	Normal*	Normal	Normal*
iPS (IMR90)-1	mTeSR1	Normal*	Normal*	Normal*	Normal*
HES3	mTeSR1	Normal*	Normal*	Normal*	Normal
KhES-1	mTeSR1	46, xx, add(13)[1]	46, xx, add(13)[13]	Normal*	Normal*
253G1	mTeSR1	Normal	Normal	Normal	Normal
H9	StemPro	Normal*	Normal*	Normal*	Normal*
iPS (IMR90)-1	StemPro	Normal	Normal	Normal	Normal*
HES3	StemPro	Normal*	Normal	Normal*	Normal*
KhES-1	StemPro	Normal	Normal*	Normal*	Normal*
253G1	StemPro	Normal	Normal	Normal	Normal
H9	N2B27	Normal	Normal	Normal	Normal
iPS (IMR90)-1	N2B27	Normal*	Normal*	Normal*	Normal*
HES3	N2B27	Normal*	Normal	Normal*	Normal
KhES-1	N2B27	Normal	Normal	Normal	Normal
253G1	N2B27	Normal	Normal	Normal	Normal

The table lists the abnormalities found in 50 randomly selected G-banded cells from tenth passage cultures.
*Indicates that a single defect of one chromosome was observed, suggesting that it may have been due to technical/procedural issues.

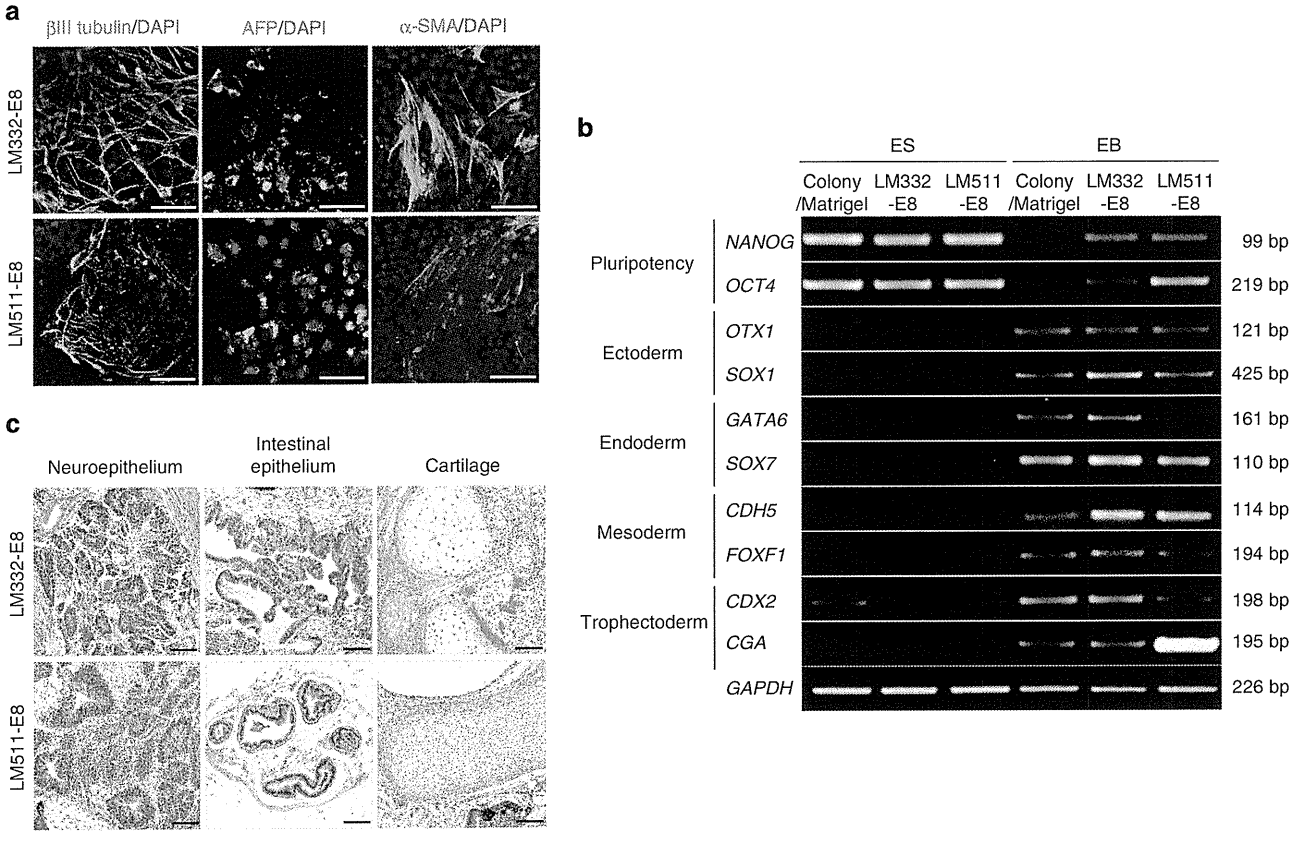

Figure 4 | LM-E8s sustain pluripotency in defined medium. (**a**) Immunostaining for markers of the three germ layers in differentiating H9 hESCs cultured on LM-E8s in mTeSR1 medium after 10 passages: ectoderm (βIII tubulin), endoderm (alpha-fetoprotein (AFP)), and mesoderm (α-smooth muscle actin (SMA)). (**b**) RT-PCR analysis of marker genes for the differentiation of embryoid bodies. H9 hESCs were cultured in mTeSR1 medium for 10 passages on LM-E8s after complete dissociation, or on Matrigel after colony dissociation. Cells were then allowed to form embryoid bodies for 10 days. (**c**) Teratomas consisting of the three germ layers developed following the transfer of H9 hESCs cultured on LM-E8s after 25 passages in mTeSR1 medium. Cells were injected into the testes of SCID mice. After 8 weeks, the fate of the cells was analysed. Haematoxylin and eosin staining showed differentiation into various tissues including neuroepithelium (ectoderm), intestinal epithelium (endoderm) and cartilage (mesoderm). Scale bars, 200 μm.

cultured on LM-E8s after complete dissociation showed that the expression of pluripotency markers, including *NANOG* and *OCT4*, remained high, whereas the expression of differentiation lineage markers was suppressed (Fig. 5c and Supplementary Fig. S6b). H9 hESCs and 253G1 iPSCs had a normal karyotype after 35 and 10 serial passages, as indicated by G-band analysis (Supplementary Fig. S7a–d), and M-FISH analysis corroborated these findings (Supplementary Fig. S7e,f). In addition, we

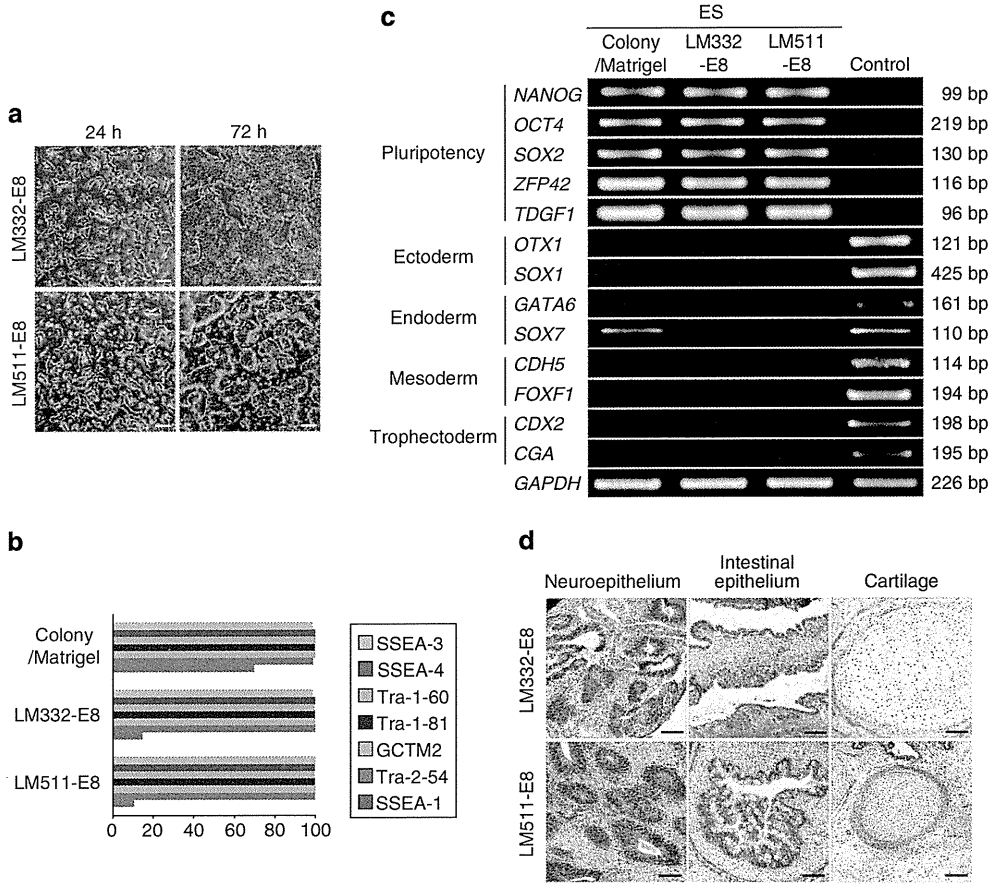

Figure 5 | LM-E8s sustain the pluripotency in xeno-free TeSR2 medium. (**a**) Phase-contrast images of H9 hESCs. Dissociated H9 hESCs in TeSR2 medium reformed clusters (24 h) and actively proliferated (72 h). (**b**) Flow cytometric profiles of H9 hESCs cultured on LM-E8s for 34 passages after complete dissociation, or on Matrigel for 30 passages after colony dissociation. H9 hESCs maintained expression of markers of the undifferentiated state. Numbers indicate percentages of cells that were positive for surface markers. (**c**) RT-PCR analysis of the expression of pluripotency marker genes in H9 hESCs cultured in TeSR2 medium. H9 hESCs cultured for 30 passages on LM-E8s after complete dissociation maintained high-level expression of pluripotency marker genes, while differentiation lineage marker genes were suppressed. Embryoid bodies derived from H9 hESCs cultured as colonies in mTeSR1 medium were used as the control to assess differentiation. (**d**) Teratomas consisting of the three germ layers developed from H9 hESCs cultured on LM-E8s for 34 passages in TeSR2 medium after complete dissociation. Cells were injected into the testes of SCID mice. After 8 weeks, the fate of the cells was analysed. Haematoxylin and eosin staining showed differentiation into various tissues including neuroepithelium (ectoderm), intestinal epithelium (endoderm) and cartilage (mesoderm). Scale bars, 200 μm.

confirmed the pluripotency of hESCs cultured on LM-E8s by their ability to form teratomas comprising all three germ layers (Fig. 5d).

Discussion

Stem cell–ECM interactions are important for maintaining stem cell adhesion, survival and self-renewal both *in vivo* and *in vitro*. The development of an ECM that sustains hESC and hiPSC cultures still requires substantial effort, particularly to avoid the use of feeder cells. In this study, we have demonstrated that LM-E8s support stronger adhesion of hESCs and hiPSCs than do other substrates, including Matrigel and intact laminin-511. We showed that LM-E8s enabled rapid and steady expansion of these cells. Furthermore, the cells cultured on LM-E8s for more than 30 passages in defined xeno-free media maintained an undifferentiated state and retained a normal karyotype and pluripotency. The adhesion of these cells to LM-E8s is primarily α6β1 integrin-dependent, because a function-blocking antibody against α6β1 integrin strongly inhibits the cell adhesion. Furthermore, LM511(EQ), a mutant LM-E8 that cannot bind to α6β1 integrin owing to a single amino-acid substitution[29], does not support the adhesion of hESCs. Thus, we believe that the interaction of LM-E8s with α6β1 integrin is the principal route for binding to hESCs and promotion of proliferation in an undifferentiated state.

Although laminin-511 was shown to be a potential substrate for feeder-free culture of hESCs, intact laminin-511 is a large heterotrimeric protein of 780 kDa (Fig. 1a) and requires three independent transfections of expression vectors encoding the α, β and γ chains, each of which is larger than 10 kb, for recombinant protein production. It is therefore an arduous protocol to produce recombinant laminin-511 in sufficient quantities for the clinical application of hESCs. Here, we have shown that LM-E8s, the minimum structure harbouring the full integrin-binding activity of laminins, are superb substrates for the long-term culture of hESCs, with a substantial advantage over intact laminin-511 and laminin-332. LM-E8s are much smaller and easier to produce recombinantly than intact laminins. Indeed, the smaller size of LM-E8s significantly improves recombinant protein expression, allowing LM-E8s to yield more than five times more recombinant protein than intact laminin-511 (see Methods). In addition, LM-E8s can be easily purified using 6xHis- and FLAG-tags attached to the α and γ chains, respectively (Fig. 1a). This method reduces the time required

for purification and increases the purity of recombinant proteins, compared with intact laminin-511. These advantages endow LM-E8s with a greater potential for scaled-up production, compared with intact laminins. Importantly, LM-E8s have a higher adhesion affinity for hESCs than do intact laminin-511 and laminin-332, although the reasons for this property are yet to be fully determined. The smaller size of LM-E8s may allow them to pack more closely to each other on the substrate and thereby increases the adhesiveness of the substrate for hESC attachment by either increasing the ligand-binding affinity of integrins and/or enhancing the signalling events triggered by integrin clustering.

Several groups have reported that vitronectin and one of its variants (VTN-NC) supports the maintenance of hESCs via αVβ5 integrin[4,13]. The binding affinity of vitronectin to αVβ5 integrin was 10-fold lower than that of LM-E8 to α6β1 integrin (Yuya Sato, K.S., unpublished data), suggesting that vitronectin is potentially inferior for hESC adhesion compared with LM-E8s. Indeed, although hESCs and hiPSCs have been cultured as colonies on fibronectin and vitronectin[1,13,35,36], hESCs and hiPSCs that had been completely dissociated showed less adhesion (Fig. 2a). It has been reported that AKT, ERK1/2 and kinases interacting with FAK are highly phosphorylated in human pluripotent stem cells[37]. Furthermore, it is well known that AKT and FAK, stimulated via integrin activation, perform numerous cell survival functions[34]. The phosphorylation of AKT, FAK and ERK1/2 confirms that LM-E8s have the potential to promote the survival of completely dissociated hESCs by robust adhesion via integrins, whereas vitronectin and fibronectin are unfavourable for culturing of completely dissociated hESCs and hiPSCs. The ROCK inhibitor Y-27632 has been shown to increase the survival of dissociated hESCs[33]. Tsutsui *et al.*[5] reported maintenance of hESCs on a fibronectin-coated surface by dissociated cell passaging, but their method requires a high dose of Y-27632 for cell attachment to fibronectin. It should be noted that a high concentration of Y-27632 increases toxicity and leads to a reduction of hESC numbers in some cases[38]. Additionally, the maintenance of hESCs on fibronectin requires constant administration of Y-27632, even after cell attachment. In contrast, our method using LM-E8s does not require Y-27632 administration owing to sufficient stimulation of cell survival from the culture substrate. This method might be advantageous not only for supporting cell expansion but also for use in drug screening studies. This is because LM-E8s not only improve the culture condition to avoid transient adverse effects of untargeted chemicals, such as Y-27632, but also allow uniform seeding of routine numbers of hESCs and hiPSCs. Therefore, LM-E8s are an appropriate culture substrate for the culture of completely dissociated hESCs and hiPSCs. Although LM-E8s ensured hESC survival just after cell seeding, single hESCs exhibited poor survival over prolonged time periods, even on LM-E8s. It is known that E-cadherin signalling, which arises from cell–cell contact, has a key role in the self-renewal of hESCs as well as the generation of hiPSCs[39–41]. LM-E8 signalling may be insufficient for prolonged survival of single hESCs, but LM-E8s enabled hESCs to actively migrate, and the cells aggregated promptly and restored cell–cell contacts to form small colonies within 24 h of culture initiation (Figs 2b, c and 5a). FAK is known to perform multiple functions and regulates cell migration[42]. The increased phosphorylation of FAK is indicative of active migration of dissociated hESCs on LM-E8s. It has been recently reported that cell–cell contact promotes hESC survival, and Y-27632 treatment accelerates the migration of hESCs to reconstruct cell–cell contacts[43]. Here, we show that LM-E8s also activated dissociated hESC migration, but the mechanism is different from that of Y-27632 treatment, as shown by the MLC2 phosphorylation analysis. Collectively, LM-E8s support not only strong adhesion to hESCs and hiPSCs but also promote cell–cell contact by inducing their migration ability, thereby ensuring cell survive and proliferation. Thus, our new protocol improves the adhesion of hESCs and hiPSCs and allows efficient propagation in a simple and rapid manner.

In conclusion, we demonstrate a defined xeno- and feeder-free culture system for hESCs and hiPSCs. LM-E8s derived from laminin isoforms support increased adhesion, survival, self-renewal and differentiation of hESCs. This simple culture system should facilitate bulk proliferation of hESCs and hiPSCs under defined xeno-free conditions. We believe that our protocol will be useful for clinical applications of hESCs and hiPSCs in compliance with good manufacturing practice and/or current good tissue practice.

Methods

Preparation of ECMs. Recombinant human laminins, laminin-111, -332 and -511 and LM-E8s (LM322-E8 and LM511-E8) were produced using a FreeStyle 293 Expression System (Invitrogen) as described previously[21,29,30]. Laminin-111, -332 and -511 and LM-E8s were filtered through 0.22-μm-pore-sized Ultrafree-CL Centrifugal Filter Units (Millipore) for sterilization. Using these methods, we purified an average of 0.74 mg intact LM511 ($n = 5$) and 4.1 mg LM511-E8 ($n = 4$) from 1 l of culture supernatant. Thus, the yield was much higher for LM511-E8 (5.5-fold in terms of weight, or 27.7-fold per mol) than for intact laminin. Furthermore, purification of intact laminin-511 required 1–2 weeks, whereas purification of LM-E8s required only 2–3 days.

Human fibronectin and vitronectin were purified from plasma, as described elsewhere[44,45]. Matrigel (Growth Factor Reduced) was purchased from BD Biosciences.

Coating of matrices. For the dose–response binding assay, 96-well flat-bottomed plates (non-treated, BD Falcon) were precoated with each of the matrices at a concentration of 0–25 μg cm^{-2} for 3 h at room temperature just before cell seeding. For other experiments, we used 48-well plates (non-treated, BD Falcon) precoated with LM-E8s, fibronectin, or vitronectin at 1.5 μg cm^{-2} or Matrigel at 25 μg cm^{-2} for 3 h at room temperature for the culture of hESCs and hiPSCs. For conventional colony passaging as an experimental control, 12-well plates were coated with Matrigel at 25 μg cm^{-2}. Coated dishes were not rinsed with buffer before use. To dilute the ECMs, Dulbecco's PBS was used for laminin-111, -332 and -511, LM-E8s, fibronectin and vitronectin. DMEM/F12 was used to dilute Matrigel.

Preparation of defined media. Commercially available defined media, mTeSR1 (mTeSR1; Stem Cell Technologies) and StemPro hESC SFM (StemPro, Invitrogen) and xeno-free medium, TeSR2 (TeSR2; Stem Cell Technologies), were used according to the manufacturer's instructions and freshly prepared every day. N2B27 medium was prepared daily, according to previous reports[1,2], and was composed of DMEM/F12 (Sigma, D6421), 1 × N2 supplement (Invitrogen), 1 × B27 supplement (Invitrogen), 1 mM non-essential amino acids (Sigma, M7145), 1 mM L-glutamine (Sigma, G7513), 0.1 mM 2-mercaptoethanol (Invitrogen) and 100 ng ml^{-1} FGF-2 (Wako, Japan, 060-04543).

Cell culture. hESC lines, KhES-1 at passage 22 and HES3 at passage 100, and hiPSC line 253G1 at passage 50 were maintained as previously described on mitomycin-C-treated mouse embryonic fibroblast (MEF) feeder cells[46]. The hESC line H9 (WA09) at passage 36, hiPSC line iPS (IMR90) clone 1 (iPS(IMR90)-1) at passage 80 and iPS (foreskin) line at passage 64 were purchased from the National Stem Cell Bank. Cells were maintained in accordance with National Stem Cell Bank protocols, except for the use of mitomycin-C-treated MEFs from the ICR strain at a density of 3.2 × 10^4 cells per cm^2.

Experimental control cells were obtained from conventional colony cultures that were maintained as follows. Near-confluent cells were incubated with 2 mg ml^{-1} dispase in DMEM/F12 at 37 °C for 2 min, and then rinsed twice with DMEM/F12. After addition of defined medium, weakly adherent colonies were detached using a cell scraper. Cells were collected and centrifuged at 200 *g* for 3 min at 4 °C. Small colonies were then passaged into Matrigel-coated vessels at a ratio of 1:4. Colonies showing morphological differentiation were manually removed under a microscope during each passage, except at the time of analysis. Completely dissociated cells were cultured after preculture in the appropriate defined medium for one passage on Matrigel-coated dishes to remove MEF feeders. This stage was defined as passage 0. Near-confluent cell clusters were treated with 4.8 mM EDTA/PBS for 2–5 min at room temperature and then TrypLE Select (Invitrogen) for 1 min at 37 °C. Cells in defined medium were pipetted to disperse the cells completely. After centrifugation at 200 *g* for 3 min at 4 °C, cells were seeded at the appropriate density (5 × 10^4 cells per cm^2 for passaging or as indicated) into new culture vessels

precoated with each matrix. The medium was changed daily for all experiments. hESCs and hiPSCs on LM-E8s were subcultured every 4–6 days, and those on Matrigel every 6–8 days.

Time-lapse recording. For time-lapse recording during initial attachment, completely dissociated H9 hESCs were seeded onto LM-E8-, fibronectin-, vitronectin- or Matrigel-coated 35-mm dishes at 2.5×10^4 cells per cm^2 in mTeSR1 medium. Recording began at 5 min after cell seeding and continued for 24 h. Movies were edited using AxioVisio software.

Cell adhesion assay. Dose–response binding assays were performed using a protocol described elsewhere[13], with some modification. Briefly, hESCs or hiPSCs were cultured for one passage on Matrigel in mTeSR1 medium to remove feeder cells, and then the cells were detached using TrypLE Select, collected and counted. A total of 5×10^4 cells were seeded into each well of 96-well plates coated with the matrices described above. After 6 h of incubation, non-adherent cells were removed by rinsing the plates twice with DMEM/F12, and the remaining adherent cells were fixed with 10% formalin for 15 min, and postfixed in 100% ethanol for 5 min at room temperature. Cells were then stained with 0.4% crystal violet in methanol for 5 min at room temperature. After washing extensively with demineralized water, the remaining cells were solubilized by adding 100 µl of 1% SDS, and the optical density at 570 nm was measured by a multiwell plate reader. For the functional inhibition assay of integrins, H9 hESCs were seeded into each well of 96-well plates coated with the various matrices including LM511(EQ) in the presence or absence of 2 µg ml^{-1} integrin-blocking antibodies, anti-α6 integrin (R&D systems) and/or anti-β1 integrin (R&D systems). After 30 min of incubation, adherent cells were screened as described above for the dose–response assay.

For the seeding density assay, hESCs or hiPSCs were precultured in mTeSR1 medium on Matrigel-coated vessels for one passage to remove feeder cells. Cells were detached using an EDTA solution and TrypLE Select as described above. Cells were seeded into 48-well plates coated with LM-E8s or Matrigel. After 6 h of incubation, non-adherent cells were rinsed twice with prewarmed DMEM/F12, and the remaining adherent cells were detached using 0.25% Trypsin/EDTA. Viable cells were counted by trypan blue exclusion.

For the proliferation assay, dissociated single cells were seeded at a density of 4×10^4 cells per cm^2, and viable cells were counted every 24 h as described above. In parallel, colonies were seeded on 24-well plates coated with Matrigel at the same cell density.

To evaluate Y-27632 pretreatment, H9 hESCs cultured on Matrigel in mTeSR1 medium were incubated with 10 µM Y-27632 (Wako, 253-00513) for 1 h just before cell detachment. Together with the cultures without Y-27632 pretreatment, cells were detached by EDTA and TrypLE Select treatment and then seeded in multiwell plates coated with substrates in mTeSR1 medium containing 10 µM Y-27632.

To evaluate the effect of Y-27632 treatment on cell proliferation, H9 hESCs after complete dissociation or as colonies were seeded at a density of 5×10^4 cells per cm^2 with or without 10 µM Y-27632 in 48-well plates coated with each substrate. Viable cells were counted every 24 h. To evaluate a derivation of vitronectin, a Synthemax-R Surface 6-well plate (Corning) was used as a substrate.

Flow cytometric analysis. Cells were dissociated by treatment with 4.8 mM EDTA/PBS for 2–5 min, followed by further treatment with a 0.05% trypsin/EDTA solution for 1 min. After two washes with DMEM/10% FBS and one wash with staining buffer (0.1% BSA/PBS), 1×10^5 cells were incubated for 30 min at 4 °C with primary antibodies diluted in staining buffer. Cells were then rinsed twice with staining buffer and incubated for 30 min at 4 °C with secondary antibodies diluted in staining buffer. Then, cells were rinsed twice with staining buffer, and counterstained with propidium iodide just before analysis.

Fluorescence intensities were analysed on a FACSCalibur flow cytometer (Becton Dickinson), and the FL-1 positive ratios in the propidium iodide-negative region were monitored using Cell Quest software. The following primary antibodies were used: SSEA-3 (2 µg ml^{-1}; Developmental Studies Hybridoma Bank (DSHB), SSEA-4 (1 µg ml^{-1}; DSHB), Tra-1-60 (1 µg ml^{-1}; Chemicon), Tra-1-81 (1 µg ml^{-1}; Chemicon), GCTM2 (1 µg ml^{-1}; Chemicon), Tra-2-54 (1 µg ml^{-1}, DSHB), and SSEA-1 (2 µg ml^{-1}; DSHB). Anti-mouse Ig/FITC conjugated (10 µg ml^{-1}; Becton Dickinson) and anti-rat IgM/Alexa 488 conjugated (1 µg ml^{-1}; Molecular Probes) were used as secondary antibodies.

Karyotyping. hESCs and hiPSCs were treated with 100 ng ml^{-1} colcemid (Invitrogen) for 2–3 h. After dissociation in 0.25% trypsin/EDTA solution, cells were treated with a hypotonic solution and then fixed in Carnoy's solution. Cells were spread onto glass slides and stained with Giemsa. Chromosome spreads were analysed by randomly counting 50 cells using the Ikaros Karyotyping System (META system). M-FISH analysis was performed using the 24XCyte Human Multicolor FISH (mFISH) Probe Kit (META system) following the manufacturer's instructions, and analysed by ISIS software (META system).

Statistical analysis. The statistical significance of differences was determined by the two-tailed Student's *t*-test for two group comparisons, or two-way analysis of variance (two-way ANOVA) for multiple comparisons followed by Tukey's test. Differences with a value of $P < 0.05$ were considered significant.

Other methods. See Supplementary Methods and Supplementary Table S2 for remaining methods, including semi-quantitative RT–PCR, the differentiation assay, immunofluorescence staining and immunoblotting.

References

1. Liu, Y. *et al.* A novel chemical-defined medium with bFGF and N2B27 supplements supports undifferentiated growth in human embryonic stem cells. *Biochem. Biophys. Res. Commun.* **346,** 131–139 (2006).
2. Akopian, V. *et al.* Comparison of defined culture systems for feeder cell free propagation of human embryonic stem cells. *In Vitro Cell Dev. Biol. Anim.* **46,** 247–258 (2010).
3. Ludwig, T. E. *et al.* Derivation of human embryonic stem cells in defined conditions. *Nature Biotech.* **24,** 185–187 (2006).
4. Chen, G. *et al.* Chemically defined conditions for human iPSC derivation and culture. *Nat. Methods* **8,** 424–429 (2011).
5. Tsutsui, H. *et al.* An optimized small molecule inhibitor cocktail supports long-term maintenance of human embryonic stem cells. *Nat. Commun.* **2,** 167 (2011).
6. Baker, M. Stem cells in culture: defining the substrate. *Nat. Methods* **8,** 293–297 (2011).
7. Thomson, J. A. *et al.* Embryonic stem cell lines derived from human blastocysts. *Science* **282,** 1145–1147 (1998).
8. Amit, M. *et al.* Clonally derived human embryonic stem cell lines maintain pluripotency and proliferative potential for prolonged periods of culture. *Dev. Biol.* **227,** 271–278 (2000).
9. Pyle, A. D., Lock, L. F. & Donovan, P. J. Neurotrophins mediate human embryonic stem cell survival. *Nature Biotech.* **24,** 344–350 (2006).
10. Draper, J. S. *et al.* Recurrent gain of chromosomes 17q and 12 in cultured human embryonic stem cells. *Nature Biotech.* **22,** 53–54 (2004).
11. Mitalipova, M. M. *et al.* Preserving the genetic integrity of human embryonic stem cells. *Nature Biotechnol.* **23,** 19–20 (2005).
12. Rodin, S. *et al.* Long-term self-renewal of human pluripotent stem cells on human recombinant laminin-511. *Nature Biotechnol.* **28,** 611–615 (2010).
13. Braam, S. R. *et al.* Recombinant vitronectin is a functionally defined substrate that supports human embryonic stem cell self-renewal via alphavbeta5 integrin. *Stem Cells* **26,** 2257–2265 (2008).
14. Melkoumian, Z. *et al.* Synthetic peptide-acrylate surfaces for long-term self-renewal and cardiomyocyte differentiation of human embryonic stem cells. *Nature Biotechnol.* **28,** 606–610 (2010).
15. Villa-Diaz, L. G. *et al.* Synthetic polymer coatings for long-term growth of human embryonic stem cells. *Nature Biotech.* **28,** 581–583 (2010).
16. Mei, Y. *et al.* Combinatorial development of biomaterials for clonal growth of human pluripotent stem cells. *Nat. Mater.* **9,** 768–778 (2010).
17. Klim, J. R., Li, L., Wrighton, P. J., Piekarczyk, M. S. & Kiessling, L. L. A defined glycosaminoglycan-binding substratum for human pluripotent stem cells. *Nat. Methods* **7,** 989–994 (2010).
18. Saha, K. *et al.* Surface-engineered substrates for improved human pluripotent stem cell culture under fully defined conditions. *Proc. Natl Acad. Sci. USA* **108,** 18714–18719 (2011).
19. Miner, J. H. & Yurchenco, P. D. Laminin functions in tissue morphogenesis. *Annu. Rev. Cell Dev. Biol.* **20,** 255–284 (2004).
20. Miyazaki, T. *et al.* Recombinant human laminin isoforms can support the undifferentiated growth of human embryonic stem cells. *Biochem. Biophys. Res. Commun.* **375,** 27–32 (2008).
21. Ido, H. *et al.* Molecular dissection of the alpha-dystroglycan- and integrin-binding sites within the globular domain of human laminin-10. *J. Biol. Chem.* **279,** 10946–10954 (2004).
22. Smirnov, S. P. *et al.* Contributions of the LG modules and furin processing to laminin-2 functions. *J. Biol. Chem.* **277,** 18928–18937 (2002).
23. Doi, M. *et al.* Recombinant human laminin-10 (alpha5beta1gamma1). Production, purification, and migration-promoting activity on vascular endothelial cells. *J. Biol. Chem.* **277,** 12741–12748 (2002).
24. Kortesmaa, J., Yurchenco, P. & Tryggvason, K. Recombinant laminin-8 (alpha(4)beta(1)gamma(1)). Production, purification,and interactions with integrins. *J. Biol. Chem.* **275,** 14853–14859 (2000).
25. Kariya, Y. *et al.* Efficient expression system of human recombinant laminin-5. *J. Biochem.* **132,** 607–612 (2002).
26. Vuoristo, S. *et al.* Laminin isoforms in human embryonic stem cells: synthesis, receptor usage and growth support. *J. Cell Mol. Med.* **13,** 2622–2633 (2009).
27. Nishiuchi, R. *et al.* Ligand-binding specificities of laminin-binding integrins: a comprehensive survey of laminin-integrin interactions using recombinant alpha3beta1, alpha6beta1, alpha7beta1 and alpha6beta4 integrins. *Matrix Biol.* **25,** 189–197 (2006).
28. Meng, Y. *et al.* Characterization of integrin engagement during defined human embryonic stem cell culture. *FASEB J.* **24,** 1056–1065 (2010).

29. Ido, H. *et al.* The requirement of the glutamic acid residue at the third position from the carboxyl termini of the laminin gamma chains in integrin binding by laminins. *J. Biol. Chem.* **282,** 11144–11154 (2007).
30. Taniguchi, Y. *et al.* The C-terminal region of laminin beta chains modulates the integrin binding affinities of laminins. *J. Biol. Chem.* **284,** 7820–7831 (2009).
31. Deutzmann, R. *et al.* Cell adhesion, spreading and neurite stimulation by laminin fragment E8 depends on maintenance of secondary and tertiary structure in its rod and globular domain. *Eur. J. Biochem.* **191,** 513–522 (1990).
32. Takagi, J. Structural basis for ligand recognition by integrins. *Curr. Opin. Cell Biol.* **19,** 557–564 (2007).
33. Watanabe, K. *et al.* A ROCK inhibitor permits survival of dissociated human embryonic stem cells. *Nature Biotech.* **25,** 681–686 (2007).
34. Vachon, P. H. Integrin signaling, cell survival, and anoikis: distinctions, differences, and differentiation. *J. Signal Transduct.* **2011,** 738137 (2011).
35. Prowse, A. B. *et al.* Long term culture of human embryonic stem cells on recombinant vitronectin in ascorbate free media. *Biomaterials* **31,** 8281–8288 (2010).
36. Lu, J., Hou, R., Booth, C. J., Yang, S. H. & Snyder, M. Defined culture conditions of human embryonic stem cells. *Proc. Natl Acad. Sci. USA* **103,** 5688–5693 (2006).
37. Phanstiel, D. H. *et al.* Proteomic and phosphoproteomic comparison of human ES and iPS cells. *Nat. Methods* **8,** 821–827 (2011).
38. Andrews, P. D. *et al.* High-content screening of feeder-free human embryonic stem cells to identify pro-survival small molecules. *Biochem. J.* **432,** 21–33 (2010).
39. Xu, Y. *et al.* Revealing a core signaling regulatory mechanism for pluripotent stem cell survival and self-renewal by small molecules. *Proc. Natl Acad. Sci. USA* **107,** 8129–8134 (2010).
40. Redmer, T. *et al.* E-cadherin is crucial for embryonic stem cell pluripotency and can replace OCT4 during somatic cell reprogramming. *EMBO Rep.* **12,** 720–726 (2011).
41. Chen, T. *et al.* E-cadherin-mediated cell-cell contact is critical for induced pluripotent stem cell generation. *Stem Cells* **28,** 1315–1325 (2010).
42. Schaller, M. D. Cellular functions of FAK kinases: insight into molecular mechanisms and novel functions. *J. Cell Sci.* **123,** 1007–1013 (2010).
43. Li, L. *et al.* Individual cell movement, asymmetric colony expansion, rho-associated kinase, and E-cadherin impact the clonogenicity of human embryonic stem cells. *Biophys. J.* **98,** 2442–2451 (2010).
44. Sekiguchi, K. & Hakomori, S. Domain structure of human plasma fibronectin. Differences and similarities between human and hamster fibronectins. *J. Biol. Chem.* **258,** 3967–3973 (1983).
45. Yatohgo, T., Izumi, M., Kashiwagi, H. & Hayashi, M. Novel purification of vitronectin from human plasma by heparin affinity chromatography *Cell Struct. Funct.* **13,** 281–292 (1988).
46. Suemori, H. *et al.* Efficient establishment of human embryonic stem cell lines and long-term maintenance with stable karyotype by enzymatic bulk passage. *Biochem. Biophys. Res. Commun.* **345,** 926–932 (2006).

Acknowledgements

We thank Ms Mari Hamao and Ms Ritsuko Goto for their valuable technical assistance and the members of the laboratories of N.N. and K.S. for insightful discussions. This work was supported by the New Energy and Industrial Technology Development Organization (NEDO) of Japan, and partially supported by the Coordination, Support and Training Programme for Translational Research of the Ministry of Education, Culture, Sports, Science and Technology of Japan (to K.S.).

Author contributions

T.M., K.S. and E.K. designed research, T.M., S.F., Y.T., M.Y., M.K., M.H. and H.K. performed research, T.M., H.S., N.N., K.S. and E.K. analysed data and T.M., K.S. and E.K. wrote the paper.

Additional information

Supplementary Information accompanies this paper at http://www.nature.com/naturecommunications

Competing financial interests: The authors declare no competing financial interests.

Reprints and permission information is available online at http://npg.nature.com/reprintsandpermissions/

How to cite this article: Miyazaki, T. *et al.* Laminin E8 fragments support efficient adhesion and expansion of dissociated human pluripotent stem cells. *Nat. Commun.* 3:1236 doi: 10.1038/ncomms2231 (2012).

RESEARCH COMMUNICATION

The SMAD2/3 corepressor SNON maintains pluripotency through selective repression of mesendodermal genes in human ES cells

Norihiro Tsuneyoshi,[1] Ee Kim Tan,[1] Akila Sadasivam,[1] Yogavalli Poobalan,[1] Tomoyuki Sumi,[2,3] Norio Nakatsuji,[4,5] Hirofumi Suemori,[2] and N. Ray Dunn[1,6]

[1]Institute of Medical Biology, A*STAR (Agency for Science, Technology, and Research), Singapore 138648, Singapore; [2]Department of Embryonic Stem Cell Research, Institute for Frontier Medical Sciences, Kyoto University, Kyoto 606-8507, Japan; [3]Department of Developmental Biology, Graduate School of Medical Sciences, Kyushu University, Fukuoka 812-8582, Japan; [4]Department of Development and Differentiation, Institute for Frontier Medical Sciences, Kyoto University, Kyoto 606-8507, Japan; [5]Institute for Integrated Cell-Material Sciences (WPI-iCeMS), Kyoto University, Kyoto 606-8501, Japan

Activin/Nodal signaling via SMAD2/3 maintains human embryonic stem cell (hESC) pluripotency by direct transcriptional regulation of *NANOG* or, alternatively, induces mesoderm and definitive endoderm (DE) formation. In search of an explanation for these contrasting effects, we focused on SNON (SKIL), a potent SMAD2/3 corepressor that is expressed in hESCs but rapidly down-regulated upon differentiation. We show that SNON predominantly associates with SMAD2 at the promoters of primitive streak (PS) and early DE marker genes. Knockdown of SNON results in premature activation of PS and DE genes and loss of hESC morphology. In contrast, enforced SNON expression inhibits DE formation and diverts hESCs toward an extraembryonic fate. Thus, our findings provide novel mechanistic insight into how a single signaling pathway both regulates pluripotency and directs lineage commitment.

Supplemental material is available for this article.

Received July 23, 2012; revised version accepted September 28, 2012.

Since the isolation of human embryonic stem cells (hESCs) more than a decade ago, numerous extrinsic signals have been implicated in the maintenance of their cardinal features of pluripotency and indefinite self-renewal (Pera and Tam 2010). These include growth factors belonging to the TGFβ, FGF, WNT, and IGF families, which are often supplemented with culture medium containing serum, feeder cell-conditioned medium, and/or ill-defined knockout serum replacement (Price et al. 1998). These various and complex platforms have obscured the identification of the minimal complement of extracellular cues that govern the intrinsic transcriptional regulators of pluripotency and self-renewal. Recently, however, it was shown that either recombinant TGFβ1 or the related ligand Activin A in combination with FGF2 can maintain hESCs in chemically defined and feeder-free conditions partly through direct regulation of the core pluripotency factor gene *NANOG* (Xu et al. 2008; Vallier et al. 2009).

Both TGFβ and Activin signals are transduced intracellularly by phosphorylation of the cytoplasmic effector proteins SMAD2 and SMAD3 (Schmierer and Hill 2007). Once activated, they partner with SMAD4, translocate to the nucleus, and associate with tissue-specific transcription factors to regulate batteries of target genes. Chromatin immunoprecipitation (ChIP) experiments show that SMAD2/3 bind the *NANOG* promoter, and luciferase reporter assays confirm that this SMAD-binding element (SBE) is crucial for *NANOG* transcriptional activity (Xu et al. 2008; Vallier et al. 2009). Recently, SMAD2/3 ChIP combined with next-generation sequencing (ChIP-seq) revealed that, in addition to *NANOG*, SMAD2/3 occupy a broad number of genes both expressed in hESCs and associated with the maintenance of pluripotency (Brown et al. 2011; Kim et al. 2011). These include the additional core pluripotency factors *OCT4* and *SOX2* as well as other key regulators, such as *SUZ12*, *UTF1*, *TERT*, *DPPA4*, and *LIN28A*. Taken together, these findings emphasize the importance of continuous TGFβ/Activin signaling for the maintenance of hESC pluripotency. However, it is a third divergent TGFβ-related ligand, Nodal, that carries out this fundamental activity in vivo.

Nodal transcripts identify the pluripotent cells within the mouse blastocyst inner cell mass (ICM) and persist in these cells as they extensively reorganize into the cup-shaped epiblast epithelium after implantation (Mesnard et al. 2006; Arnold and Robertson 2009). In the absence of *Nodal*, null mutant embryos down-regulate *Oct4*, *Nanog*, and *Foxd3*, which are normally uniformly expressed throughout the epiblast; prematurely and ectopically up-regulate neural markers; and fail to gastrulate (Camus et al. 2006; Mesnard et al. 2006). With the onset of gastrulation, *Nodal* expression resolves to the posterior primitive streak (PS), where epiblast cells ingress and emerge as mesoderm and definitive endoderm (DE) (Arnold and Robertson 2009). Extensive genetic studies have shown that the highest levels of Nodal specify DE, while the assorted mesodermal lineages are patterned by intermediate to lower Nodal levels (Arnold and Robertson 2009). Thus, there is a remarkable conversion in a narrow developmental time span in how Nodal signals are interpreted intracellularly—from maintenance of pluripotency within the ICM/epiblast to inducer of differentiation within the PS. This raises the intriguing question of how Nodal/Smad2/3 signals in the ICM/epiblast engage only the pluripotency machinery and avert precocious activation of differentiation genes. This question also stringently applies to hESCs, which share many defining characteristics with the mouse epiblast and its derivative cell lines (termed epiblast stem cells [EpiSCs]) (Pera and Tam 2010),

[*Keywords*: Activin/Nodal; SNON; human embryonic stem cells; mesendoderm; pluripotency; repressor]
[6]**Corresponding author**
E-mail ray.dunn@imb.a-star.edu.sg
Article is online at http://www.genesdev.org/cgi/doi/10.1101/gad.201772.112.

as the Nodal analog Activin A both regulates pluripotency and is nearly universally used to initiate mesendoderm differentiation in vitro to produce a variety of lineage-specific cell types (Sulzbacher et al. 2009).

We reasoned that one explanation for these contrasting effects is the existence of discriminating nuclear repressor proteins. Moreover, the expression of such a repressor would likely be under the direct control of the core pluripotency factors. Previous ChIP combined with DNA microarrays (ChIP–chip) identified numerous active and inactive genes that are triply bound by OCT4, SOX2, and NANOG in hESCs (Boyer et al. 2005). One of these is the SKI-related proto-oncogene *SNON* (*SKIL*) that encodes a potent negative regulator of TGFβ-related signaling (Deheuninck and Luo 2009; Zhu and Luo 2012). SNON physically interacts with SMAD2, SMAD3, and SMAD4, disrupting their assembly into an activated heteromeric complex (Stroschein et al. 1999; Wu et al. 2002). In addition, SNON prevents SMAD2 and SMAD3 from associating with the transcriptional coactivator p300/CBP and recruits a repressor complex comprised of nuclear receptor corepressor (N-CoR) and histone deacetylase (HDAC) (Schmierer and Hill 2007). Thus, the presence of SNON at a particular SBE ensures transcriptional repression. Here, we found that SNON protein is highly abundant in hESCs and specifically enriched at differentiation gene promoters. Loss of SNON in hESCs prematurely activates PS and early DE genes and destabilizes pluripotency, while constitutive SNON expression restrains differentiation into DE. Taken together, our results identify SNON as a key component of the nuclear machinery that safeguards pluripotency through direct repression of differentiation genes downstream from Activin/Nodal.

Results and Discussion

SNON is abundant in hESCs and is targeted to the proteasome during early differentiation

We first sought to confirm the expression of *SNON* in pluripotent hESCs and examine its regulation during DE formation in vitro. Differentiation was carried out according to the schematic in Figure 1A (Teo et al. 2012) and, expectedly, resulted in the loss of pluripotency markers (*NANOG*, *OCT4*, and *SOX2*) and up-regulation of PS (*WNT3*, *FGF8*, *EOMES*, and *MIXL1*), mesendoderm (*GSC* and *LHX1*), and DE (*FOXA2* and *SOX17*) markers by day 5 (Supplemental Fig. 1A). These data were confirmed by Western analysis, immunohistochemistry, and FACS (Supplemental Fig. 1B–D). We observed that *SNON* transcript levels are robust in undifferentiated HES3 and on day 1 of differentiation but drop considerably by day 3 and decline further on day 5 (Fig. 1B).

This decrease in *SNON* levels in vitro closely mirrors the expression dynamics of *SnoN* in the early mouse embryo. Prior to gastrulation, *SnoN* transcripts label the pluripotent epiblast epithelium (Supplemental Fig. 1E). Mouse ESCs and EpiSCs also express *SnoN* (Supplemental Fig. 1F). With the onset of gastrulation, *SnoN* transcript levels are conspicuously down-regulated in the region of the incipient PS and continue to decline posteriorly as the PS lengthens (Supplemental Fig. 1E). Nascent mesoderm and DE also lack *SnoN* expression. By the late PS stage (embryonic day 7.5 [E7.5]), *SnoN* transcripts resolve to the anterior epiblast, but shortly

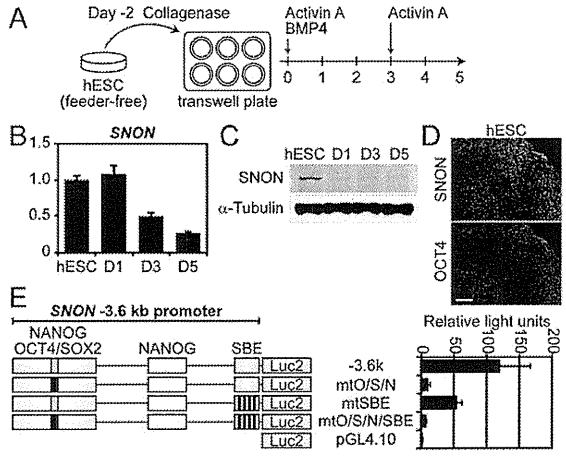

Figure 1. *SNON* expression in hESCs is controlled by SMAD2/3 and OCT4, SOX2, and NANOG. (*A*) hESCs were differentiated into DE for 5 d according to the schematic. Activin A and BMP4 (both at 50 ng/mL) were added on day 0. Only Activin A was replenished on day 3. (*B*) *SNON* expression levels during DE differentiation by qPCR. Data were normalized against *GUSB* and are shown relative to undifferentiated hESCs (= 1.0). (*C*) Western blot analysis for SNON protein levels during DE differentiation. (*D*) OCT4 and SNON immunofluorescence on undifferentiated HES3 (hESCs). Bar, 100 μm. (*E*) Luciferase reporter assays of *SNON* promoter activity in HES3. Black shading indicates specific mutation of the OCT4/SOX2/NANOG-binding sites in the 5′ distal enhancer or of the four SBEs proximal to the *SNON* transcriptional start site.

thereafter, this domain has largely disappeared. These expression data suggest that loss of the Smad2/3 corepressor SnoN is an obligate step in the production of PS-derived lineages.

At the protein level, SNON is abundant in undifferentiated HES3 but, in contrast to our quantitative PCR (qPCR) data, drastically reduced by day 1 (Fig. 1C,D). SKI, which is closely related to SNON, is also present in hESCs, but its levels fluctuate negligibly between days 1 and 5 (Supplemental Fig. 1B,G). Several E3 ubiquitin ligases previously shown to target SNON to the proteasome are expressed in hESCs and during differentiation, including SMURF2, the RING domain-containing protein ARKADIA (RNF111), and the anaphase-promoting complex/cyclosome (APC/C) (Deheuninck and Luo 2009). *SMURF2* levels are up-regulated on day 1 and then plateau, while expression of *ARKADIA* and two APC/C subunits—*CDH1* (*FZR1*) and *ANAPC2*—increase gradually (Supplemental Fig. 1G). Similar results were observed by Western for SMURF2 and ARKADIA (Supplemental Fig. 1B). Other APC/C components, including *ANAPC11*, *CDC16*, and *CDC27*, were equally expressed at all time points (Supplemental Fig. 1G).

To confirm that the rapid loss of SNON protein is indeed due to proteasomal degradation, feeder-free HES3 cells were treated with two proteasome inhibitors: MG132 and lactacystin. When HES3 cells are differentiated in the presence of MG132 or lactacystin, SNON protein levels expectedly persist on day 1 (Supplemental Fig. 1H). Taken together, these data show that *SNON* expression is tightly linked to pluripotency and that SNON is targeted to the proteasome at the onset of DE formation.

SNON *expression in hESCs is controlled by SMAD2/3 and OCT4, SOX2, and NANOG*

ChIP–chip, recent ChIP-seq, and phylogenetic alignments reveal a series of conserved SMAD2/3- and OCT4/SOX2/NANOG-binding regions within the ~5-kb *SNON* promoter/enhancer (Fig. 1E; Supplemental Fig. 1I; Boyer et al. 2005; Zhu et al. 2005; Brown et al. 2011; Kim et al. 2011). We investigated the contribution of each of these elements to *SNON* regulation in undifferentiated hESCs using luciferase reporter constructs. Serial deletion analysis showed that the distal 5′ OCT4/SOX2/NANOG-binding region is essential for robust reporter activity (Supplemental Fig. 1I). The more proximal NANOG and SMAD2/3 elements contribute modestly to the regulation of *SNON* when compared with the −3.6-kb construct (Supplemental Fig. 1I). We also generated a series of −3.6-kb reporters in which OCT4/SOX2/NANOG- and SMAD2/3-binding sites were individually mutated (Fig. 1E; Supplemental Table 1). Consistent with our deletion studies, the mutated OCT4/SOX2/NANOG (mtO/S/N) construct in which distal OCT4/SOX2/NANOG binding is specifically disrupted shows significantly reduced (~13-fold) reporter activity (Fig. 1E). In contrast, mutating all four SBEs (mtSBEs) diminishes *SNON* reporter activity roughly twofold (Fig. 1E). Taken together, these data establish that *SNON* is TGFβ-responsive and that OCT4/SOX2/NANOG serve as critical upstream regulators of *SNON* expression in hESCs.

SNON knockdown destabilizes pluripotency

To analyze SNON function, we first performed tetracycline (Tet)-inducible shRNA-mediated knockdown of *SNON* in S4TR5 cells, a derivative of the Shef4 hESC line that constitutively expresses the nuclear Tet repressor (TetRnls) (Zafarana et al. 2009). Two independent and previously validated human SNON-shRNA target sequences—shSNON(954) and shSNON(1307)—were transfected into S4TR5 cells (Sarker et al. 2005; Zhu et al. 2007). After selection, 11 of 12 clones for shSNON(954) and 10 of 12 clones for shSNON(1307) showed ~80% *SNON* knockdown by qPCR after 3 d of doxycycline (Dox) treatment (data not shown). Two clones, designated shSNON(954) and shSNON(1307), were chosen for further study. Both were indistinguishable by morphology (Supplemental Fig. 2A) and showed OCT4, SOX2, and NANOG levels comparable with the parental S4TR5 line by qPCR and Western (Supplemental Fig. 2B,C). Dox treatment resulted in a significant knockdown of *SNON* transcripts on day 1 (Fig. 2A,B). Interestingly, both shSNON clones lost their compact colony morphology after 5 d of continuous culture in Dox and appeared differentiated (Supplemental Fig. 2A). This was accompanied by a specific increase in PS (*BRACHYURY*, *MIXL1*, and *EOMES*), mesendoderm (*GSC*), and early DE (*FOXA2* and *SOX17*) markers beginning around day 3 (Fig. 2B; Supplemental Fig. 2B). Neuroectodermal gene expression was not above background (Supplemental Fig. 2B) and, importantly, levels of *OCT4*, *SOX2*, and *NANOG* remained unchanged (Supplemental Fig. 2B,C). In addition, loss of SNON did not impact SKI, SMURF2, SMAD2/pSMAD2, or SMAD3/pSMAD3 levels, suggesting that the genes encoding these proteins are not regulated by the SNON corepressor in hESCs (Supplemental Fig. 2C). Consistent with our qPCR data, Western analysis

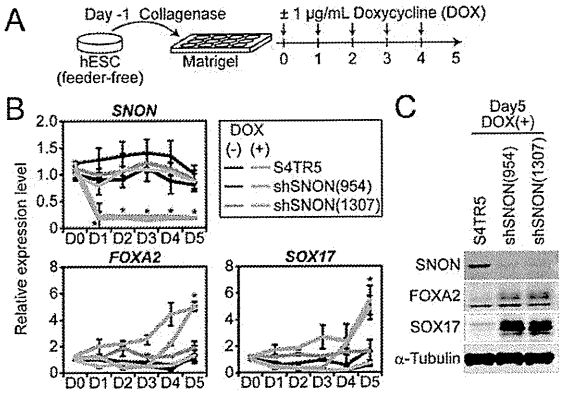

Figure 2. SNON knockdown induces differentiation in hESCs. (*A*) Schematic of the experimental design using two stable DOX-inducible S4TR5 hESC lines—shSNON(954) and shSNON(1307)—where DOX was replenished daily for 5 d. (*B*) *SNON*, *FOXA2*, and *SOX17* expression analysis by qPCR. RNA was collected on days 0–5 according to *A*. Data were normalized against *GUSB* and are depicted relative to S4TR5 (DOX−) at day 0 (= 1.0). *P*-values were calculated according to the Student's *t*-test. (*) $P < 0.05$. (*C*) Western blot analysis for SNON, FOXA2, and SOX17.

revealed that SNON is hardly detectable on day 1, and low levels of FOXA2 were first detected on day 2, followed by SOX17 on day 5 (Fig. 2C; Supplemental Fig. 2D). Immunofluorescence also confirmed loss of SNON, persistence of OCT4, and up-regulation of SOX17 and FOXA2 on day 5 (Supplemental Fig. 2E,F).

To provide additional evidence that loss of SNON results in differentiation, we performed a replating experiment whereby S4TR5 cells and both knockdown clones were passaged after 5 d of Dox treatment and cultured for four additional days in Dox. OCT4-DAB staining was used to identify hESC colonies and clearly revealed the dramatically reduced plating efficiency of the shSNON knockdown clones after passaging (Supplemental Fig. 2G). Taken together, our results show that diminished SNON levels in hESCs destabilizes pluripotency through precocious activation of mesendodermal genes.

SNON overexpression blocks differentiation into DE and mesoderm

We next performed the reciprocal experiment by overexpressing *SNON* in hESCs. After repeated attempts, we were unable to isolate HES3 subclones with levels greater than endogenous SNON (data not shown). We therefore chose to overexpress a stable truncated form of SNON—SNON(1–366)—that retains its ability to bind SMAD2/3 and is sufficient for transcriptional repression but lacks the C-terminal lysine resides critical for ubiquitination and proteasomal degredation (Stroschein et al. 1999, 2001). Two SNON(1–366) clones (#1 and #9) were isolated that produce roughly equivalent levels of SNON(1–366) (Fig. 3A) and remain undifferentiated, with OCT4 immunoreactivity comparable with wild-type HES3 (Supplemental Fig. 3A).

Clones #1 and #9 were then subjected to DE differentiation according to the schematic in Figure 1A, along with two controls: wild-type HES3 and HES3 harboring pCAG-IRES-puro (vector control). *NANOG*, *OCT4*, *SOX2*, and *DPPA4* levels declined with similar kinetics in controls

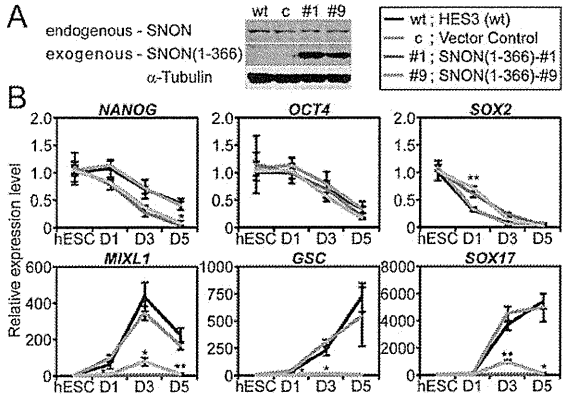

Figure 3. SNON overexpression inhibits DE formation. (*A*) Western blot analysis detects abundant C-terminally truncated, constitutively active SNON(1–366) in two stable, clonally selected lines (#1 and #9). (*B*) Expression analysis of the indicated genes by qPCR. hESCs were differentiated according to the schematic in Figure 1A. Data were normalized against *GUSB* and are shown relative to parental wild-type undifferentiated hESCs (= 1.0). The "vector control" HES3 line contains only the pCAG-IRES-Puro construct. *P*-values were calculated according to the Student's *t*-test. (*) $P < 0.05$; (**) $P < 0.01$.

and clones #1 and #9 (Fig. 3B; Supplemental Fig. 3C). HES3 and the vector control cell line predictably showed up-regulation of the PS markers (*BRACHYURY, WNT3, FGF8, MIXL1,* and *EOMES*) as well as mesendodermal (*LHX1* and *GSC*) and DE (*FOXA2* and *SOX17*) markers beginning on day 1 (Fig. 3B; Supplemental Fig. 3C). Clones #1 and #9 failed to activate the expression of PS, mesendodermal, and DE marker genes, all of which are known Activin/Nodal targets and bound by SMAD2/3 (Fig. 3B; Supplemental Fig. 3C; Schmierer and Hill 2007; Arnold and Robertson 2009). This result is entirely consistent with the ability of SNON(1–366) to strongly suppress the synthetic ARE-lux Activin/Nodal pathway reporter, which contains three repeats of a *Xenopus* Activin response element (ARE) that binds SMAD2/4 and the forkhead transcription factor FOXH1. Human GSC-Luc2 and MIXL1-Luc2 reporters containing their respective endogenous AREs are similarly repressed by SNON(1–366) (Supplemental Fig. 3D). When confronted with culture conditions tailored to produce cardiomyocytes (Hudson et al. 2012), SNON(1–366)-overexpressing clones also fail to up-regulate early mesodermal progenitor markers (Supplemental Fig. 3E). SNON(1–366) therefore serves as a potent inhibitor of both mesoderm and DE formation downstream from Activin/Nodal signals. Consequently, SNON(1–366)-expressing clones initiate extraembryonic lineage differentiation in response to Activin A and BMP4 treatment, as evidenced by the up-regulation of the trophoblast marker genes *CDX2, CGA, CYP19A, GCM1, KRT7, LGALS16,* and *VGLL1* and the visceral/parietal endoderm marker *SOX7* (Supplemental Fig. 3C). In addition, no induction of early neuroectodermal markers (*NEUROD1* and *SOX1*) was observed (Supplemental Fig. 3C).

SNON occupies SBEs in mesendodermal genes

To formally test whether SNON binds and represses PS and mesendodermal genes in undifferentiated hESCs, we performed SMAD2, SMAD3, and SNON ChIP followed by qPCR for enrichment at select SBEs. Given the high percentage of amino acid identity between SMAD2 and SMAD3 and the potential for antibody cross-reactivity, we used monoclonal anti-SMAD2 and anti-SMAD3 antibodies that specifically distinguish between these two proteins (Supplemental Figs. 1K, 4B). Among "stem cell factor" genes (*NANOG, OCT4, SOX2, DPPA4,* and *LIN28*) that are highly expressed in hESCs, SNON occupancy at their respective SBEs was low to undetectable (Fig. 4A; Supplemental Fig. 4A). Only *SUZ12* showed statistically significant enrichment for SNON ($P < 0.05$). However, *SUZ12,* like the other stem cell factor genes analyzed, was insensitive to SNON(1–366) overexpression (Supplemental Fig. 3C). In contrast, SNON highly occupied PS (*FGF8, WNT3, EOMES,* and *MIXL1*) and mesendodermal (*GSC* and *LHX1*) genes (Fig. 4A; Supplemental Fig. 4A). SMAD2 bound all SBEs analyzed by ChIP (Fig. 4A; Supplemental Fig. 4A). Consistent with the ability of SNON to recruit HDACs, acetylated H3 and H4 levels at PS/mesendodermal genes were low in undifferentiated HES3 cells but increased with differentiation (Supplemental Fig. 4C; Xi et al. 2011). The converse was observed at stem cell factor gene promoters, with declining acetylation mirroring the decrease in pluripotency gene expression during differentiation (Supplemental Figs. 1A, 3C, 4C). Taken together, these data are wholly consistent with SNON in combination with SMAD2/SMAD4 acting as a key transcriptional repressor of differentiation-specific genes in pluripotential hESCs (Fig. 4B).

Our ChIP data also reveal a bias of SMAD3 toward stem cell factor gene promoters (Fig. 4A; Supplemental Fig. 4A). In a very recent study, Mullen et al. (2011) reported that OCT4 and SMAD3 are predominantly associated with transcriptionally active genes in hESCs and, importantly, co-occupy the genome by binding adjacent DNA sites. Our results show that no repression of pluripotency genes was observed in hESC clones overexpressing SNON(1–366), which retains its ability to bind SMAD3 but cannot be targeted by E3 ligases (Fig. 3B; Supplemental Fig. 3C). These genes include *NANOG,* whose regulation by TGFβ/Activin/SMAD2/3 in hESCs is extremely well characterized (Xu et al. 2008; Vallier et al. 2009). If SNON were a general repressor downstream from TGFβ-related signaling, modulating the overall activity of the TGFβ pathway in hESCs, ectopic expression of SNON(1–366) would be predicted to suppress *NANOG* and other crucial pluripotency genes and promote differentiation. This is not what we observed (Fig. 3B; Supplemental Fig. 3D). We therefore propose that OCT4 serves a central "protective" role in averting SNON repression of SMAD3-bound pluripotency genes (Fig. 4B). In contrast, selective recruitment of SNON represses PS/mesendoderm genes in hESCs until extrinsic cues trigger its degradation and allow differentiation to unfurl.

One outstanding question is thus the identity of the E3 ligases specifically responsible for the rapid clearance of SNON at the onset of differentiation. Genetic evidence in mice favors a role for Arkadia because *Arkadia*-null mutant embryos succumb to severe gastrulation defects due to impaired Nodal/Smad2/3 signaling (Episkopou et al. 2001; Mavrakis et al. 2007). One interpretation of this phenotype is that in the absence of Arkadia, SnoN associates with crucial Nodal/Smad2/3 target genes,

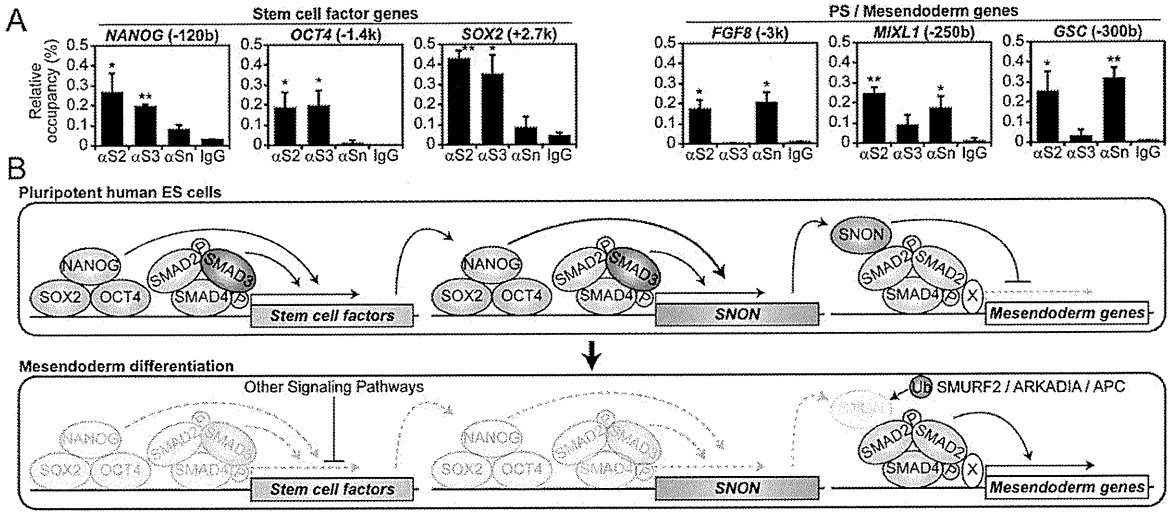

Figure 4. SNON highly and selectively occupies the promoters of PS and mesendodermal genes in hESCs. (*A*) ChIP-qPCR analysis of SNON-binding (αSn), SMAD2-binding (αS2), and SMAD3-binding (αS3) sites at the indicated gene regions in HES3 cultured in mTeSR1 medium. Relative occupancy values are shown as the apparent immunoprecipitation efficiency (percentage) (ratio = immunoprecipitated DNA/input DNA). (IgG) Normal rabbit IgG as negative control. *P*-values were calculated according to the Student's *t*-test. (*) $P < 0.05$; (**) $P < 0.01$. (*B*) Proposed model for SNON function in hESCs. In pluripotent hESCs, extrinsic signals (e.g., TGFβ/Activin/Nodal) regulate stem cell factor gene expression through activated SMAD2/3/4 complexes. OCT4/SOX2/NANOG positively regulate their own promoters and activate *SNON* transcription. SMAD2/3 also regulate *SNON*. SNON is selectively recruited to SMAD2-bound mesendodermal genes and suppresses their transcription. During early differentiation, stem cell factor gene expression and SMAD2/3/4 occupancy at the SNON promoter/enhancer decline. Consequently, *SNON* expression decreases. Existing SNON protein is rapidly degraded in a ligand-dependent manner by E3 ubiquitin ligases (e.g., SMURF2, ARKADIA, or APC). This leads to the derepression of early PS and DE target genes (collectively referred to as mesendoderm). (X) Tissue-specific transcriptional coactivators such as FOXH1.

preventing their activation. Consistent with this prediction, SnoN protein accumulates in *Arkadia*-deficient mouse ESC lines (Nagano et al. 2007). Thus, SNON degradation in hESCs may similarly require the stimulus-dependent activation of ARKADIA or the synergistic involvement of other ligand-dependent E3 ligases, such as SMURF2 (Bonni et al. 2001). It is important to note that there are >600 E3 ligases and substrate recognition subunits encoded by the human genome (Li et al. 2008), many of which are enriched in hESCs (Assou et al. 2009). This finding presages the heightened sensitivity that hESCs exhibit to proteasome inhibitors (Assou et al. 2009; Vilchez et al. 2012; data not shown) and further suggests that there are additional hitherto uncharacterized regulators that act alongside ARKADIA, APC, and SMURF2 to target SNON to the proteasome.

Materials and methods

Cell culture

HES3 cells were maintained as previously described (Suemori et al. 2006). For feeder-free culture, HES3 and S4TR5 cells (Zafarana et al. 2009) were maintained in mTeSR1 medium (Stem Cell Technologies) on 1:200 GFR-Matrigel-coated (Becton Dickinson) dishes. DE differentiation was carried out as previously described (Teo et al. 2012).

Tet-inducible shRNA knockdown

Previously validated human *SNON* shRNA target sequences were ligated into pSUPERIOR-Zeocin (Supplemental Material; Sarker et al. 2005; Zhu et al. 2007). S4TR5 cells were transfected with the shRNA constructs using FuGene HD (Roche) and selected for 2 wk using 2.5 μg/mL Zeocin (Invitrogen).

SNON overexpression

Human *SNON*(1–366) cDNA was PCR-amplified and ligated into pCAG-IRES-Puro (Supplemental Material; Sumi et al. 2007). Feeder-free HES3 cells were transfected with pCAG-SNON(1–366)-IRES-Puro or empty vector using FuGene HD and selected for 2 wk using 1 μg/mL puromycin (Sigma).

qPCR analysis

Total RNA was extracted using the RNeasy kit (Qiagen), and 0.5–2 μg was reverse-transcribed with the High-Capacity cDNA Reverse Transcription kit (Applied Biosystems). Real-time PCR was performed using TaqMan Fast Advanced Master Mix or Power SYBR Green PCR Master Mix. Relative quantitation was performed using $2^{-\Delta\Delta CT}$ and normalized against *GUSB*. TaqMan gene expression assays and primers are listed in Supplemental Table 2.

Luciferase assay

An ~5-kb segment of the human *SNON* promoter was PCR-amplified (Supplemental Table 1) and subcloned into pGL4.10[*luc2*] (Promega). pTK-*hRluc* was used for data normalization (Supplemental Material). Molar equivalents of each *luc2* reporter vector and 0.05 μg of pTK-*hRluc* were cotransfected into HES3 using FuGene HD. After 48 h, both firefly and *Renilla* luciferase activities were measured using the Dual-Luciferase Reporter Assay system (Promega). Relative luciferase units were calculated by determining the ratio between firefly and *Renilla* luciferase activities and normalizing against the pGL4.10 vector control.

Immunofluorescence and immunocytochemical analysis

For immunofluorescence, hESCs were fixed in 3.7% formaldehyde/PBS for 15 min, permeabilized with 0.2% Triton X-100/PBS for 5 min, and incubated with primary antibodies (Supplemental Table 3). After incubation with Alexa Fluor 488- or 594-conjugated secondary antibodies

(Invitrogen), nuclei were counterstained with DAPI (Sigma). For immunocytochemical staining of OCT4, hESCs were fixed, permeabilized, and incubated with anti-OCT4 antibody (Supplemental Table 3). After incubation with HRP-conjugated secondary antibody (Dako), antigens were visualized with DAB (Sigma).

Western blot analysis

Cell lysates were separated by SDS-PAGE, transferred to Immobilon-FL PVDF membrane (Millipore), and probed with primary antibodies (Supplemental Table 3). After incubation with IRDye 800CW- or 680LT-conjugated secondary antibodies (LI-COR), proteins were detected using the Odyssey infrared imaging system (LI-COR).

ChIP and quantitative real-time PCR

ChIP was performed as described previously (Boyer et al. 2005). Additional details are provided in the Supplemental Material.

Acknowledgments

We thank Stuart Avery and Peter Andrews for providing S4RT5 cells, Ludovic Vallier for mEpiSC RNA, and Alan Colman, Dmitry Bulavin, Leah Vardy, Matthew Lovatt, Oz Pomp, Elizabeth Robertson, Elizabeth Bikoff, and Oliver Dreesen for insightful discussions and comments on the manuscript.

References

Arnold SJ, Robertson EJ. 2009. Making a commitment: Cell lineage allocation and axis patterning in the early mouse embryo. *Nat Rev Mol Cell Biol* **10:** 91–103.

Assou S, Cerecedo D, Tondeur S, Pantesco V, Hovatta O, Klein B, Hamamah S, De Vos J. 2009. A gene expression signature shared by human mature oocytes and embryonic stem cells. *BMC Genomics* **10:** 10. doi: 10.1186/1471-2164-10-10.

Bonni S, Wang HR, Causing CG, Kavsak P, Stroschein SL, Luo K, Wrana JL. 2001. TGF-β induces assembly of a Smad2-Smurf2 ubiquitin ligase complex that targets SnoN for degradation. *Nat Cell Biol* **3:** 587–595.

Boyer LA, Lee TI, Cole MF, Johnstone SE, Levine SS, Zucker JP, Guenther MG, Kumar RM, Murray HL, Jenner RG, et al. 2005. Core transcriptional regulatory circuitry in human embryonic stem cells. *Cell* **122:** 947–956.

Brown S, Teo A, Pauklin S, Hannan N, Cho CH, Lim B, Vardy L, Dunn NR, Trotter M, Pedersen R, et al. 2011. Activin/Nodal signaling controls divergent transcriptional networks in human embryonic stem cells and in endoderm progenitors. *Stem Cells* **29:** 1176–1185.

Camus A, Perea-Gomez A, Moreau A, Collignon J. 2006. Absence of Nodal signaling promotes precocious neural differentiation in the mouse embryo. *Dev Biol* **295:** 743–755.

Deheuninck J, Luo K. 2009. Ski and SnoN, potent negative regulators of TGF-β signaling. *Cell Res* **19:** 47–57.

Episkopou V, Arkell R, Timmons PM, Walsh JJ, Andrew RL, Swan D. 2001. Induction of the mammalian node requires Arkadia function in the extraembryonic lineages. *Nature* **410:** 825–830.

Hudson J, Titmarsh D, Hidalgo A, Wolvetang E, Cooper-White J. 2012. Primitive cardiac cells from human embryonic stem cells. *Stem Cells Dev* **21:** 1513–1523.

Kim SW, Yoon SJ, Chuong E, Oyolu C, Wills AE, Gupta R, Baker J. 2011. Chromatin and transcriptional signatures for Nodal signaling during endoderm formation in hESCs. *Dev Biol* **357:** 492–504.

Li W, Bengtson MH, Ulbrich A, Matsuda A, Reddy VA, Orth A, Chanda SK, Batalov S, Joazeiro CA. 2008. Genome-wide and functional annotation of human E3 ubiquitin ligases identifies MULAN, a mitochondrial E3 that regulates the organelle's dynamics and signaling. *PLoS ONE* **3:** e1487. doi: 10.1371/journal.pone.0001487.

Mavrakis KJ, Andrew RL, Lee KL, Petropoulou C, Dixon JE, Navaratnam N, Norris DP, Episkopou V. 2007. Arkadia enhances Nodal/TGF-β signaling by coupling phospho-Smad2/3 activity and turnover. *PLoS Biol* **5:** e67. doi: 10.1371/journal.pbio.0050067.

Mesnard D, Guzman-Ayala M, Constam DB. 2006. Nodal specifies embryonic visceral endoderm and sustains pluripotent cells in the epiblast before overt axial patterning. *Development* **133:** 2497–2505.

Mullen AC, Orlando DA, Newman JJ, Lovén J, Kumar RM, Bilodeau S, Reddy J, Guenther MG, DeKoter RP, Young RA. 2011. Master transcription factors determine cell-type-specific responses to TGF-β signaling. *Cell* **147:** 565–576.

Nagano Y, Mavrakis KJ, Lee KL, Fujii T, Koinuma D, Sase H, Yuki K, Isogaya K, Saitoh M, Imamura T, et al. 2007. Arkadia induces degradation of SnoN and c-Ski to enhance transforming growth factor-β signaling. *J Biol Chem* **282:** 20492–20501.

Pera MF, Tam PP. 2010. Extrinsic regulation of pluripotent stem cells. *Nature* **465:** 713–720.

Price PJ, Goldsborough MD, Tilkins ML. 1998. *Embryonic stem cell serum replacement*. International Patent Application WO 98/30679.

Sarker KP, Wilson SM, Bonni S. 2005. SnoN is a cell type-specific mediator of transforming growth factor-β responses. *J Biol Chem* **280:** 13037–13046.

Schmierer B, Hill CS. 2007. TGFβ-SMAD signal transduction: Molecular specificity and functional flexibility. *Nat Rev Mol Cell Biol* **8:** 970–982.

Stroschein SL, Wang W, Zhou S, Zhou Q, Luo K. 1999. Negative feedback regulation of TGF-β signaling by the SnoN oncoprotein. *Science* **286:** 771–774.

Stroschein SL, Bonni S, Wrana JL, Luo K. 2001. Smad3 recruits the anaphase-promoting complex for ubiquitination and degradation of SnoN. *Genes Dev* **15:** 2822–2836.

Suemori H, Yasuchika K, Hasegawa K, Fujioka T, Tsuneyoshi N, Nakatsuji N. 2006. Efficient establishment of human embryonic stem cell lines and long-term maintenance with stable karyotype by enzymatic bulk passage. *Biochem Biophys Res Commun* **345:** 926–932.

Sulzbacher S, Schroeder IS, Truong TT, Wobus AM. 2009. Activin A-induced differentiation of embryonic stem cells into endoderm and pancreatic progenitors-the influence of differentiation factors and culture conditions. *Stem Cell Rev* **5:** 159–173.

Sumi T, Tsuneyoshi N, Nakatsuji N, Suemori H. 2007. Apoptosis and differentiation of human embryonic stem cells induced by sustained activation of c-Myc. *Oncogene* **26:** 5564–5576.

Teo AKK, Ali Y, Wong KY, Chipperfield H, Sadasivam A, Poobalan Y, Tan EK, Wang ST, Abraham S, Tsuneyoshi N, et al. 2012. Activin and BMP4 synergistically promote formation of definitive endoderm in human embryonic stem cells. *Stem Cells* **30:** 631–642.

Vallier L, Mendjan S, Brown S, Chng Z, Teo A, Smithers LE, Trotter MW, Cho CH, Martinez A, Rugg-Gunn P, et al. 2009. Activin/Nodal signalling maintains pluripotency by controlling Nanog expression. *Development* **136:** 1339–1349.

Vilchez D, Boyer L, Morantte I, Lutz M, Merkwirth C, Joyce D, Spencer B, Page L, Masliah E, Berggren WT, et al. 2012. Increased proteasome activity in human embryonic stem cells is regulated by PSMD11. *Nature* **489:** 304–308.

Wu JW, Krawitz AR, Chai J, Li W, Zhang F, Luo K, Shi Y. 2002. Structural mechanism of Smad4 recognition by the nuclear oncoprotein Ski: Insights on Ski-mediated repression of TGF-β signaling. *Cell* **111:** 357–367.

Xi Q, Wang Z, Zaromytidou AI, Zhang XH, Chow-Tsang LF, Liu JX, Kim H, Barlas A, Manova-Todorova K, Kaartinen V, et al. 2011. A poised chromatin platform for TGF-β access to master regulators. *Cell* **147:** 1511–1524.

Xu RH, Sampsell-Barron TL, Gu F, Root S, Peck RM, Pan G, Yu J, Antosiewicz-Bourget J, Tian S, Stewart R, et al. 2008. NANOG is a direct target of TGFβ/activin-mediated SMAD signaling in human ESCs. *Cell Stem Cell* **3:** 196–206.

Zafarana G, Avery SR, Avery K, Moore HD, Andrews PW. 2009. Specific knockdown of OCT4 in human embryonic stem cells by inducible short hairpin RNA interference. *Stem Cells* **27:** 776–782.

Zhu Q, Luo K. 2012. SnoN in regulation of embryonic development and tissue morphogenesis. *FEBS Lett* **586:** 1971–1976.

Zhu Q, Pearson-White S, Luo K. 2005. Requirement for the SnoN oncoprotein in transforming growth factor β-induced oncogenic transformation of fibroblast cells. *Mol Cell Biol* **25:** 10731–10744.

Zhu Q, Krakowski AR, Dunham EE, Wang L, Bandyopadhyay A, Berdeaux R, Martin GS, Sun L, Luo K. 2007. Dual role of SnoN in mammalian tumorigenesis. *Mol Cell Biol* **27:** 324–339.